

A synthetic lethal screen identifies the Vitamin D receptor as a novel gemcitabine sensitizer in pancreatic cancer cells

V Bhattacharjee, Y Zhou, and TJ Yen*

Fox Chase Cancer Center; Institute for Cancer Research; Philadelphia, PA USA

Keywords: BXPC3, chemosensitization, DNA repair, gemcitabine, HDAC inhibitors, Panc1, pancreatic cancer, PARP inhibitor, p300, Rad51 foci, siRNA screen, stalled replication fork, Vitamin D receptor, VDR

Abbreviations: PCa, Pancreatic cancer; VDR, Vitamin D receptor; DNA DSB, DNA Double-strand break; IF, Immunofluorescence.

Overcoming chemoresistance of pancreatic cancer (PCa) cells should significantly extend patient survival. The current treatment modalities rely on a variety of DNA damaging agents including gemcitabine, FOLFIRINOX, and Abraxane that activate cell cycle checkpoints, which allows cells to survive these drug treatments. Indeed, these treatment regimens have only extended patient survival by a few months. The complex microenvironment of PCa tumors has been shown to complicate drug delivery thus decreasing the sensitivity of PCa tumors to chemotherapy. In this study, a genome-wide siRNA library was used to conduct a synthetic lethal screen of Panc1 cells that was treated with gemcitabine. A sublethal dose (50 nM) of the drug was used to model situations of limiting drug availability to PCa tumors in vivo. Twenty-seven validated sensitizer genes were identified from the screen including the Vitamin D receptor (VDR). Gemcitabine sensitivity was shown to be VDR dependent in multiple PCa cell lines in clonogenic survival assays. Sensitization was not achieved through checkpoint override but rather through disrupting DNA repair. VDR knockdown disrupted the cells' ability to form phospho- γ H2AX and Rad51 foci in response to gemcitabine treatment. Disruption of Rad51 foci formation, which compromises homologous recombination, was consistent with increased sensitivity of PCa cells to the PARP inhibitor Rucaparib. Thus inhibition of VDR in PCa cells provides a new way to enhance the efficacy of genotoxic drugs.

Introduction

Pancreatic cancer (PCa) is the 4th leading cause of cancer fatality in the United States and has the lowest 5-year survival rate of any major cancer (ACS). More than 70% of patients die within the first year after being diagnosed. By year 2020, it is anticipated that PCa will move to the 2nd leading cause of cancer death (Pancreatic Cancer Action Network, 2012). At the time of diagnosis, over 52% of the patients have distant disease and 26% have regional spread (ACS). Only ~15% of patients diagnosed with pancreatic adenocarcinoma can have their tumors surgically removed. Lack of early diagnosis, complex biology of the disease, and limited treatment options contribute in making PCa such a major killer.

Virtually all pancreatic tumors are adenocarcinomas of which the vast majority expresses a mutant K-Ras.¹⁻⁴ Over 2 decades of PCa research suggest a model for disease progression where early, low-grade pancreatic intraepithelial neoplasia (PanIN), is associated with KRAS2 mutations and telomere shortening.^{1,5} Intermediate and late stages of the disease are characterized by loss of

p16/CDKN2A, SMAD4, p53, and BRCA2 respectively.⁶ Additionally, a massive effort to sequence the genomes of 24 independently derived advanced pancreatic adenocarcinomas revealed a remarkably complex pattern of genetic mutations.² On average, there were 63 genetic mutations in PCa. The majority (67%) of the mutations could be classified into 12 partially overlapping cellular signaling pathways.

PCAs are notoriously insensitive to the backbone of cancer chemo- and radiation therapy, all of which target processes essential for the integrity of the genome. Gemcitabine, a nucleoside analog that blocks DNA replication, remains the first line therapy for patients with advanced PCa.^{7,8} The efficacy of gemcitabine over 5-fluorouracil, which had previously been the drug of choice, was based on a very modest increase in median survival of less than 2 months.⁹ Although erlotinib (EGFR inhibitor) has been approved by the FDA for PCa, it only increased survival by less than a month, when used in combination with gemcitabine.¹⁰ Therefore, gemcitabine continues to be the backbone of standard of care. FOLFIRINOX regimen consisting of multiple drugs can extend survival, but because of toxicity issues this is not

*Correspondence to: T.J. Yen; Email: Timothy.yen@fccc.edu

Submitted: 08/22/2014; Revised: 09/10/2014; Accepted: 09/11/2014

<http://dx.doi.org/10.4161/15384101.2014.967070>

be a viable option for all patients¹¹⁻¹³ since only patients with high performance status are the only ones who qualify for FOLFIRINOX. Most recently, gemcitabine and Abraxane (Nab-paclitaxel) showed a modest survival benefit compared to gemcitabine alone (median overall survival of 8.5 months vs 6.7 months) and has been approved by the FDA as a frontline combination treatment for metastatic PCa.¹⁴

Several approaches have been adopted to improve treatment strategies. One approach is to identify inhibitors that specifically target mutated oncoproteins, which can be a highly effective treatment strategy if tumor cells depend critically on oncogenic pathways.¹⁵ However, PCas that harbor KRAS mutations do not respond to farnesyl transferase inhibitors.¹⁶ Pancreatic tumors have been shown to have abundant tumor stromal content.¹⁷ Therefore, the amount of drug actually reaching the tumor is quite low. Studies in mice have shown that disrupting the stroma with inhibitors of the hedgehog signaling pathway can improve drug response.¹⁸ However, recent work from the same group has shown that disrupting the PCa stromal microenvironment actually renders tumors more aggressive, and these tumors exhibit increased vascularity and proliferation.¹⁹ The proposed reason for this discrepancy was that the increased drug delivery benefit was counteracted by increased angiogenesis, invasiveness, and metastasis of PCa tumors.

Understanding the mechanisms of chemoresistance of PCa will provide new targets that enhance cell killing by drugs such as gemcitabine. Recently, several groups have advanced the understanding of gemcitabine resistance in cancer. Gemcitabine resistant cancer cells have been shown to have undergone epithelial to mesenchymal transition (EMT).²⁰ 3-bromopyruvate has been shown to sensitize PCa cells to gemcitabine.²¹ In this study, we used a genome-wide siRNA library to perform a synthetic lethal screen to identify gemcitabine sensitizers in the Panc1 pancreatic adenocarcinoma cell line. Synthetic lethality is based on genetic studies in drosophila and yeast, where mutational disruption of 2 or more pathways is necessary to elucidate a biological process that is specified by multiple or overlapping processes.^{22,23} This method has been used on human cancers that harbor specific loss of function mutations in pathways that are involved in cellular sensitivity to cytotoxic stress.²⁴⁻²⁶

Our screen identified 27 genes that sensitized PCa cells to killing by gemcitabine. We focused on the Vitamin D receptor (VDR) because its role in chemoresistance of PCa has not previously been studied. VDR is, a nuclear hormone receptor family member that binds vitamin D ($1\alpha,25(\text{OH})_2\text{D}_3$) and regulates the expression of genes that are essential for calcium homeostasis and bone mineralization.²⁷ Although VDR is not an essential gene, it is expressed in most tissues and organs where it participates in diverse biological processes that are important for detoxification, immune functions, differentiation, and growth control.²⁸⁻³⁰ In fact, VDR is considered a target for chemoprevention cancer therapy since $1\alpha,25(\text{OH})_2\text{D}_3$ (VD3) has anti-proliferative activity against a variety of cancer cells in vitro,^{31,32} in vivo, and in clinical trials.³³⁻³⁵ However, VD3 and some of its analogs induced hypercalcemia in patients and thus limits its usefulness as a chemopreventative agent.³⁶ However, calcitriol (1,25 di hydroxy vitamin D) that does not commonly induce

hypercalcemia has been shown to promote caspase-dependent apoptosis and reduces tumor volume in combination with gemcitabine in Capan-1 pancreatic adenocarcinoma cells and tumors.³⁷ VDR expression has also been shown to be induced by DNA damage in the skin as a result UVB exposure.³⁸ VDR expression is also induced by p73 following DNA damage in human non-small lung carcinoma cells.²⁹ A positive feedback loop has been reported to exist between the DNA damage checkpoint kinase ATM and VDR following DNA damage.³⁹ Studies of MEFs with damaged DNA showed that VDR was phosphorylated by ATM which in turn promoted VDR transactivation of the ATM gene.

In this study, we show that VDR is critical for the survival of pancreatic cancer cells to gemcitabine treatment. We show that drug response correlates with the levels of VDR expression in different PCa cells. Furthermore, gemcitabine survival depends on ligand binding and dimerization domains within VDR. We demonstrate that VDR is critical for gemcitabine treated cells to recruit Rad51 and phospho- γH2AX to sites of DNA damage. VDR does not appear to dictate foci formation by regulating the expression of these genes. Instead, our data suggests that it acts through epigenetic mechanisms that regulate foci formation by Rad51. Rad51 is a critical component of the error-free homologous recombination (HR) pathway that is the major repair mechanism for stalled replication forks that is induced by gemcitabine. We believe that gemcitabine sensitization of VDR depleted cells is due to their reduced capacity to repair damaged DNA. This is supported by the observation that cells with reduced VDR levels are more sensitive to PARP inhibitors, which preferentially kill cells deficient in HR.⁴⁰

Results

A RNAi synthetic lethality screen to enhance gemcitabine sensitivity

We performed a genome-wide siRNA screen to identify genes and pathways in Panc1 pancreatic adenocarcinoma cells that can be targeted for gemcitabine sensitization. We used a sublethal dose (IC20) of gemcitabine (50 nM) that was sufficient to induce an S phase arrest and DNA damage as seen by γH2AX foci (Figure S1). The low dose of gemcitabine (50 nM) may also be clinically relevant as it has been reported that only a small percentage of a chemotherapeutic dose of drugs actually reaches the PCa tumor because of its dense stromal microenvironment.^{18,41} Two days after siRNA transfection, gemcitabine or vehicle was added to duplicate plates and cell viability was assessed 48 hours later. Values were normalized to internal standards, as each plate contained negative and positive controls, and comparisons made between vehicle and gemcitabine treated samples. Statistical analysis of the data was used to rank the siRNAs according to their ability to enhance gemcitabine killing. We determined the false discovery rate (FDR) for each sample and used a cutoff of 0.2 to identify 125 primary candidates. Candidates were further validated for gemcitabine sensitization with a set of deconvolved siRNAs (4 individual siRNAs for each gene). Twenty-seven genes were validated based on the ability of > 2 of 4 deconvolved

siRNAs to enhance gemcitabine killing (Table S1). The validated hits were subjected to pathway analysis using Ingenuity and STRING databases to assess potential relationships with one another (Figure S2A and B). Consistent with previous reports, a major gemcitabine survival network consisted of various DNA damage response genes involved in repair and checkpoint functions (Chk1, Wee1, PIAS4, and 53BP1).⁴²⁻⁴⁶ This result validated our screen and gave us confidence to further evaluate candidates not previously known to be involved in gemcitabine response.

The vitamin D receptor (VDR) sensitizes pancreatic cancer cells to gemcitabine

We focused on the Vitamin D Receptor (VDR) (Figure S2), a member of the superfamily of nuclear hormone receptors, for a number of reasons. VDR has been implicated as a biomarker for lung cancer progression,⁴⁷ and its expression in lung cancer cells is increased in response to DNA damaging agents.²⁹ In K-ras mutated colon cancer cells, VDR suppression leads to cell death mediated by p38 MAP kinase.⁴⁸ p38 activation by constitutive expression of its activator MKK6 or arsenite selectively induces cell death in K-ras mutated HCT116 cells and not in K-ras mutant disrupted HCT116-derived sublines. This selective cell death is linked to VDR downregulation by an AP-1-dependent mechanism as forced VDR expression in K-ras mutated cells render them resistant to p38 induced cell death, and inhibition of endogenous VDR in K-ras mutant disrupted cells render them sensitive. Although the role of VDR in drug sensitization has not been documented, there have been reports that suggest a relationship with DNA damage. A positive feedback loop has been reported to exist between the DNA damage checkpoint kinase, ATM, and VDR following DNA damage.³⁹ Notably, ATM and VDR expression were increased after DSB induction by N-nitroso-N-methylurea through ATM phosphorylation of VDR which in turn promoted VDR transactivation of the ATM gene. In addition, Vitamin D3 (1 α ,25(OH)₂D₃) which is the major ligand of VDR, has been shown to protect cells from genotoxic stress by promoting DNA repair. Vitamin D3 (VD3) bound VDR is responsible for clearing cyclobutane pyrimidine dimers (CPDs) and pyrimidone photoproducts (6,4 PP) in mice that were exposed to UVB.⁴⁹ Moreover, topically applied VD3 protected skin from UV induced photodamage.⁵⁰

We first compared the sensitization achieved with VDR knockdown to that of Chk1 knockdown, a well known chemosensitization target that overrides the DNA damage checkpoint and promotes mitotic catastrophe.⁵¹⁻⁵⁶ We conducted clonogenic assays as this was more sensitive and reliable than the short term viability assays. Panc1 cells transfected with control, VDR, and Chk1 siRNA's were treated with vehicle or 50 nM gemcitabine for 24 hrs before drugs were washed out and cells seeded for clonogenic assays (Fig. 1A). Colony formation did not differ significantly in control siRNA samples treated with vehicle versus gemcitabine. Compared to control samples treated with gemcitabine, only 8% and 3% of the gemcitabine treated VDR and Chk1 siRNAs transfected cells survived, respectively. Colony formation of 92% and 77% efficiency was seen for vehicle treated

VDR and Chk1 siRNAs transfected cells, respectively. We extended these studies to establish gemcitabine kill curves following control and VDR siRNA transfections of Panc1, BxPC3, and CFPAC1 cells. All 3 PCa cell lines showed increased sensitivity to gemcitabine after knockdown of VDR (Fig. 1B). BxPC3 cells treated with control siRNA had a mean IC₅₀ of ~200 nM as compared to the mean IC₅₀ of ~60 nM after transfection with VDR siRNA (p value of 0.036). CFPAC1 cells treated with control siRNA had a mean IC₅₀ of ~45 nM while the IC₅₀ of VDR depleted cells was reduced to ~20 nM (p = 0.083). Similarly, the IC₅₀ of control transfected Panc1 cells was reduced from ~30 nM to ~18 nM after VDR knockdown.

To establish specificity of the VDR siRNA, we attempted to rescue the sensitization by expressing RNAi resistant alleles of WT-VDR in cells stably knocked down of VDR. We set out to establish stable VDR knockdown cell lines by utilizing a lentiviral shRNA delivery system. BxPC3, Panc1, and CFPAC1 cells were infected with virus but only BxPC3 cells that were stably knocked down of VDR were recovered. This suggests that VDR maybe essential in Panc1 and CFPAC1 cells (see discussion). Western blots showed that BxPC3 VDRkd cells had ~10 fold reduction of VDR protein compared to the parental BxPC3 cells (Figure S3A). Vector and WT-VDR were transfected into the BxPC3 VDRkd cells (Figure S3B) and tested for gemcitabine sensitivity in clonogenic assays. As with the untransfected cells, vector transfected cells had an IC₅₀ of ~50 nM gemcitabine. However, cells transfected with WT-VDR showed increased IC₅₀ of ~300 nM gemcitabine (p = 0.089) (Fig. 1C). To extend these results, we next tested various VDR mutants that are unable to activate transcription.⁵⁷ Vitamin D3 is the major ligand that binds to VDR to activate transcription. In addition, transcription is usually mediated by a heterodimer of VDR and RXR (retinoid acid X receptor). VDR mutants defective in ligand binding and heterodimerization have been characterized extensively.⁵⁷ Mutations that disrupted ligand binding (C288G) and heterodimerization (K246G) (L254G) were transfected into the BxPC3 VDRkd cells but none of them rescued the gemcitabine sensitivity as with WT-VDR (Fig. 1D). As a further test for VDR specificity, we utilized 2 dominant negative mutants to neutralize the ability of WT-VDR to restore gemcitabine resistance to the BxPC3 VDRkd cells. The S237M mutation in VDR prevents binding by vitamin D3 but unlike other ligand mutants, it exerts a dominant negative effect by titrating away essential binding partners from endogenous VDR.⁵⁸ Additionally, we utilized the AML1/ETO fusion oncogene that also sequesters VDR from its binding partners, RXR and Runx2, thus disrupting the formation of VDR transcriptional machinery.^{59,60} When WT-VDR was co-transfected with either the S237M mutant or AML1/ETO into BxPC3 VDRkd cells, colony formation after gemcitabine treatment was reduced when compared to just WT-VDR transfected cells (Fig. 1D). The IC₅₀ for WT-VDR transfected cells was ~260 nM while co-transfection of S237M or AML1/ETO reduced the IC₅₀s to ~60 nM (p = 0.039) and ~80 nM (p = 0.147) respectively, very similar to the IC₅₀ for the untransfected VDR knockdown cells. The combined data establish that both the ligand-binding and

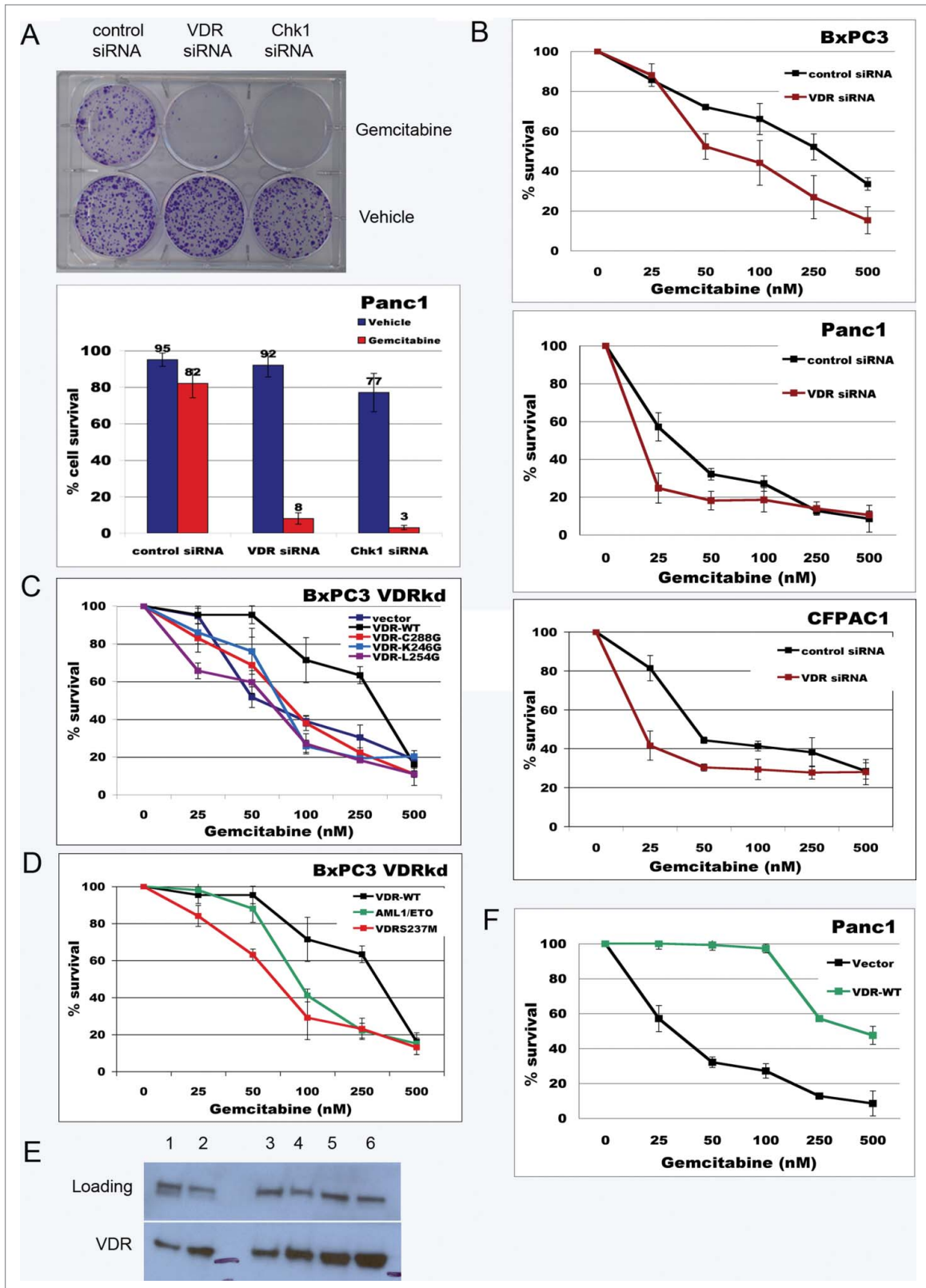


Figure 1. For figure legend, see page 3843.

heterodimerization domains are essential for VDR's role in promoting gemcitabine survival.

We next compared the levels of VDR protein in BxPC3, CFPAC1, and Panc1 cells to see if the amount of expression might correlate with gemcitabine sensitivity. Western blots showed that the basal levels of VDR differed among the cell lines such that BxPC3 had the highest amounts of VDR, followed by CFPAC1, and then Panc1 cells (Fig. 1E). After overnight treatment with gemcitabine, VDR levels increased in Panc1 and CFPAC1 cells. No noticeable increase in VDR levels was seen in BxPC3 perhaps due to its high basal level. Comparison of the gemcitabine sensitivity showed that it negatively correlated with VDR levels (Fig. 1E) such that BxPC3 cells with the highest levels of VDR had a mean IC50 of ~200 nM, while CFPAC1 and Panc1 cells had IC50s of ~45 nM and ~30 nM, respectively.

We next used Panc1 cells for VDR overexpression experiments to further test the relationship between VDR and gemcitabine sensitivity. Cells transfected with WT-VDR were significantly more resistant to gemcitabine (IC50 ~250 nM) than cells transfected with vector (IC50 ~25 nM) (Figs. 1F and S4A). The VDR overexpression data supports the VDR knockdown data in establishing that levels of VDR expression is a critical determinant for gemcitabine response in pancreatic cancer cells.

VDR specifies a survival pathway that is distinct from the DNA damage checkpoint pathway

Since VDR knockdown achieved the same degree of gemcitabine sensitization as Chk1 knockdown, we tested whether the mechanism of VDR sensitization was due to checkpoint override. We used time-lapse microscopy to track the fates of gemcitabine treated Panc1 cells that stably expressed a H2B:GFP fusion protein that labeled chromosomes. Cells were transfected with siRNAs, treated with vehicle or gemcitabine and monitored every 10 minutes for 48 hours (Figs. 2, S4B, and S4C). Control, VDR, or Chk1 siRNAs did not affect viability of vehicle treated cells as their numbers increased at the end of 48 hours. Addition of gemcitabine to control siRNA cells stopped proliferation as a result of the checkpoint, but cells did not die during the span of the time-lapse experiment. As shown previously, Chk1 knockdown abrogated the cell cycle arrest mediated by gemcitabine as cells were observed to enter mitosis where many died or died shortly after exit from mitosis.^{51,61,62} By contrast, cells transfected with VDR siRNA never entered mitosis, but nevertheless died during the

span of the ~48 hour time-lapse. Gemcitabine sensitization after VDR knockdown is therefore not due to override of the DNA damage checkpoint pathway mediated by Chk1.

VDR knockdown impairs foci formation by DNA damage response proteins γ H2AX, 53BP1, and Rad51 following gemcitabine treatment

We investigated if drug sensitization after VDR knockdown might be due to defective DNA damage repair. Gemcitabine is a nucleoside analog that acts as a chain terminator that will stall replication forks. If the forks cannot restart, they collapse to form DNA double strand breaks that can be detected by the formation of phospho- γ H2AX foci.⁶³ Repair of stalled forks is mediated by the error-free homologous recombination pathway (HR). Rad51, an essential component of HR, has been implicated in promoting gemcitabine resistance in non-small-cell lung cancer and pancreatic cancer.^{64,65} 53BP1 on the other hand protects DSB ends from resection (which is required for HR) to promote non-homologous end-joining (NHEJ) which is an error-prone repair pathway.⁶⁶ We examined if these repair pathways were abrogated after VDR knockdown by staining for foci formation by phospho- γ H2AX, Rad51, and 53BP1, and measuring intensities after gemcitabine treatment (Figs. 3–5). BxPC3 (high VDR expression) and Panc1 (low VDR expression) cells were treated with gemcitabine (50 nM) for 2, 4, 8, and 18 hours, and fixed and stained for phospho- γ H2AX, 53BP1, and Rad51. Foci quantitation included counting of nuclei with > 5 foci and a separate measurement of the sum intensities of foci that were averaged for 5 separate IF experiments. Thus, our foci counts do not reflect their intensities, which were quantitated separately. Weak but detectable phospho- γ H2AX foci were visible within 4 hours of gemcitabine treatment in BxPC3 cells while it took 18 hours for foci to form in Panc1 cells (Fig. 3A). Similarly, Rad51 foci were visible after 8 hours of gemcitabine treatment in BxPC3 cells compared to 18 hours in Panc1 cells (Figs. 3A–5). The kinetics of 53BP1 foci formation were comparable between the 2 cell lines. Next, we tested whether VDR deficiency affected the kinetics of foci formation in BxPC3 and Panc1 cells. We compared the kinetics of foci formation in the BxPC3 VDRkd cells to the foci formation observed in the parental cells. We utilized transient siRNA transfections to knockdown VDR in the Panc1 cells. VDR knockdown delayed foci formation and reduced foci intensities of phospho- γ H2AX and Rad51 in both cell lines (Figs. 3A–5). 53BP1 foci formation kinetics did not seem to be

Figure 1 (See previous page). Sensitization of pancreatic cancer cells to gemcitabine following VDR knockdown. (A) Colony formation assay comparing gemcitabine sensitivity of Panc1 cells after control, VDR and Chk1 siRNA transfection. Cells were treated with 50nM gemcitabine for 24 hrs. and drug removed before the assay. Colony counts are presented beneath the image of a representative colony survival assay. (B) Gemcitabine kill curves from clonogenic survival assays performed on BxPC3, Panc1 and CFPAC1 cells following control or VDR siRNA transfection (n = 5). p values: BxPC3 = 0.036, Panc1 = 0.171, CFPAC1 = 0.083. (C) clonogenic survival assays of gemcitabine sensitivity of BxPC3 VDRkd cells transfected with the indicated VDR constructs (n = 5). p values: VDR-WT = 0.088, VDR-C288G = 0.671, VDR-K246G = 0.845, VDR-L254G = 0.148. (D) AML1/ETO and VDR-S237M neutralizes the ability of WT-VDR to rescue gemcitabine resistance of BxPC3 VDRkd cells (n = 5). p values: AML1/ETO = 0.147, VDR-S237M = 0.039. (E) Western blot showing VDR expression after 18 hour vehicle or gemcitabine (50 nM) treatment of PCa cell lines. 40 μ g of protein loaded. Lane 1 = Panc1 + Vehicle; Lane 2 = Panc1 + gemcitabine; Lane3 = CFPAC1 + Vehicle; Lane 4 = CFPAC1 + gemcitabine; Lane 5 = BxPC3 + Vehicle; Lane 6 = BxPC3 + gemcitabine. The 55 kDa marker is labeled between lanes 2 and 3, and to the right of lane 6. (F) Increased resistance of Panc1 cells to gemcitabine following VDR overexpression (n = 5). p value = 0.008.

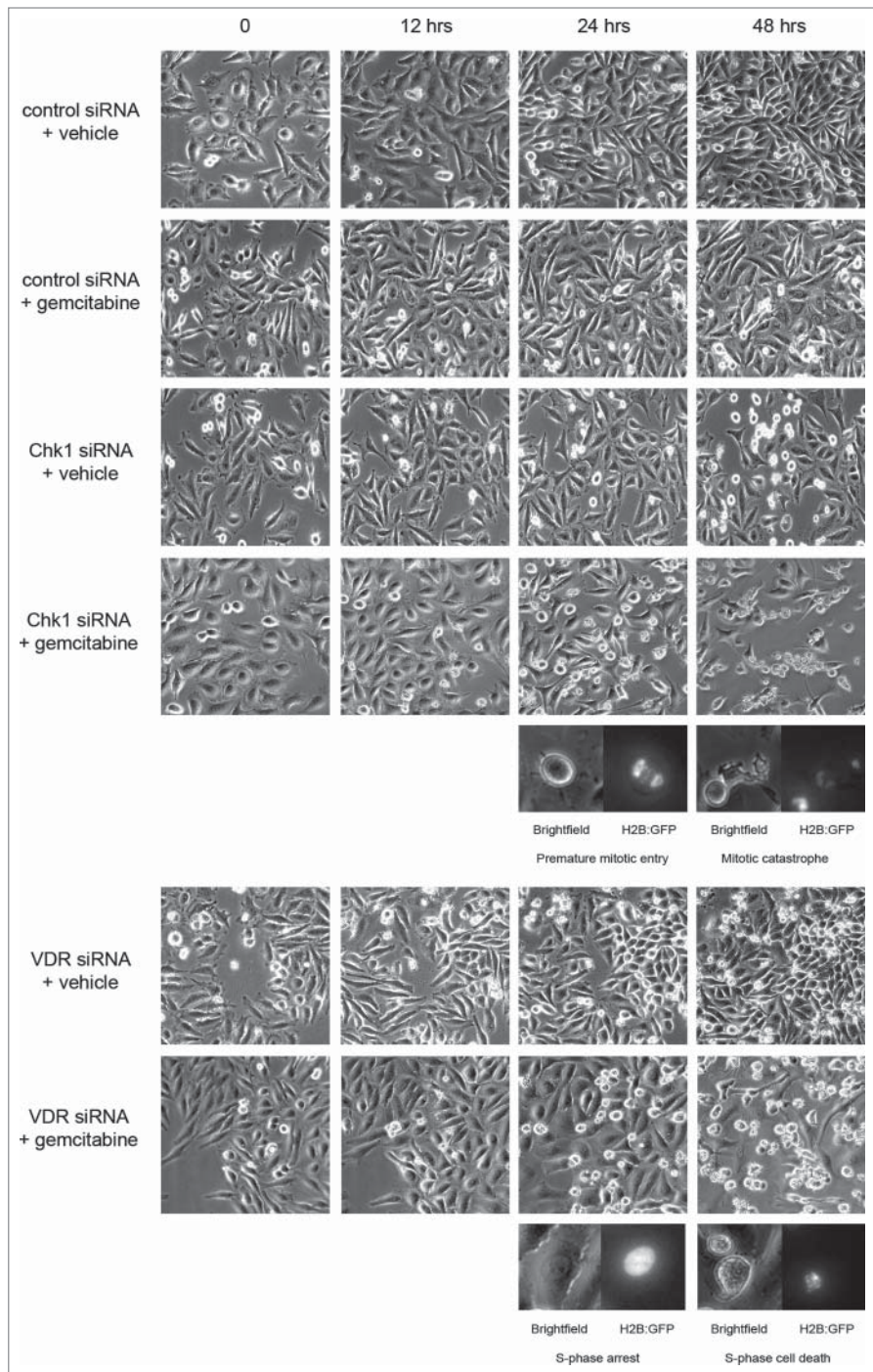


Figure 2. Gemcitabine sensitization after VDR knockdown is not due to override of the DNA damage checkpoint. Select frames from a 48 hr timelapse of Panc1 cells transfected with control, Chk1, and VDR siRNAs that were treated with vehicle or gemcitabine. Chk1 siRNA of gemcitabine treated samples show increased mitotic cells at later timepoints. Enlarged images show brightfield and gfpH2B images of Chk1 siRNA cells prematurely entering mitosis and undergoing mitotic catastrophe. VDR siRNA transfected cells remain in interphase and die without ever entering mitosis.

Along with the delayed kinetics foci formation and reduced intensities of phospho- γ H2AX and Rad51 after VDR knockdown, we noticed qualitative differences in the staining patterns of Rad51, 53BP1, and phospho- γ H2AX. Parental BxPC3 cells form discrete punctate phospho- γ H2AX foci compared to the VDRkd cells that displayed a diffuse, pan nuclear phospho- γ H2AX staining pattern (Fig. 3B). The punctate pattern is indicative of damage recognition and subsequent repair complex formation near the sites of damage.⁶⁷⁻⁶⁹ In contrast, the diffuse pattern is indicative of damage recognition, but is believed to reflect a failure to retain repair complexes distal to damage sites which leads to further accumulation of DNA damage that eventually leads to catastrophic cell death.⁶⁷⁻⁶⁹ phospho- γ H2AX formed punctate foci 18 hours after gemcitabine treatment in 94% of the parental BxPC3 cells. By contrast, punctate foci were seen in only 18% of the VDRkd cells and the remaining 82% of the cells exhibited a diffuse pattern (Fig. 3B). Although the kinetics of foci formation by 53BP1 was not affected by VDR knockdown (Fig. 3A), it also exhibited a more diffuse 53BP1 staining pattern as seen for phospho- γ H2AX (Fig. 3B). After 18 hours of gemcitabine treatment, 90% of the parental cells formed punctate 53BP1 foci and 10% expressed the diffuse pattern. This contrasts with only 31% of the VDRkd cells formed punctate foci while 69% expressed the diffuse pattern. Similarly, Rad51 foci formation was also compromised in the VDRkd cells. After 18 hours of gemcitabine treatment, 92% of the parental BxPC3 cells exhibited clear Rad51 foci as compared to 28% of the VDRkd cells. 72% of VDRkd cells (which were also phospho- γ H2AX positive) exhibited diffuse Rad51 staining as compared to only 8% that were

affected by VDR knockdown in either cell line (Figs. 3A–5). Phospho- γ H2AX and Rad51 foci in BxPC3 VDRkd cells were detected 8 and 18 hours, respectively, following addition of gemcitabine as compared to 4 and 8 hours respectively, in the parental cells. Similarly, Panc1 cells transfected with VDR siRNA did not exhibit phospho- γ H2AX and Rad51 foci until 18 hours following gemcitabine addition as compared to ~8 hours for Panc1 cells transfected with control. Importantly, the slower kinetics of foci formation in Panc1 cells was accelerated by transient VDR overexpression in Panc1 cells (Fig. 5).

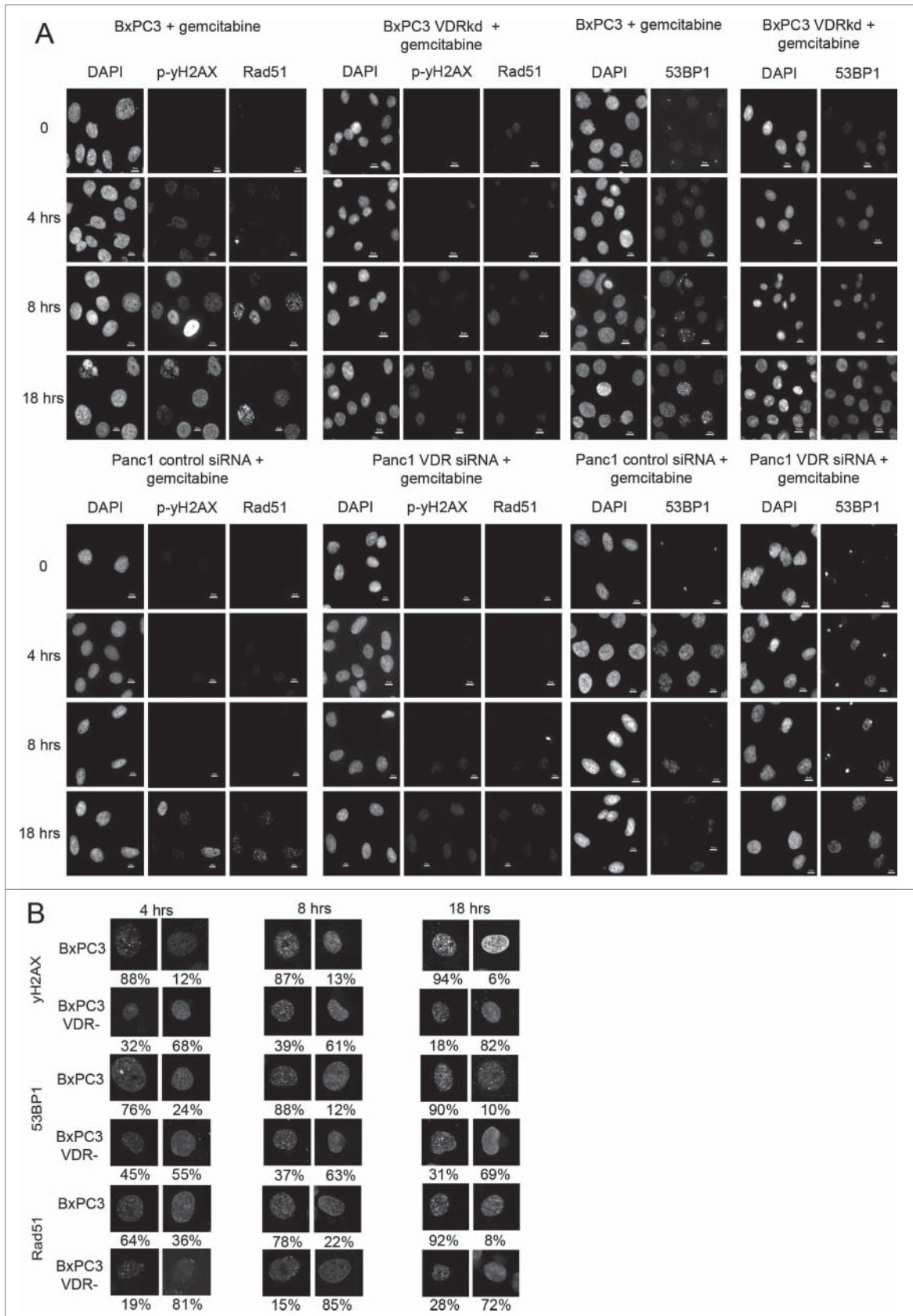


Figure 3. For figure legend, see page 3846.

seen in the parental cells (Fig. 3B). Therefore, VDR knockdown not only delays the kinetics of foci formation of phospho- γ H2AX and Rad51, but also compromises the ability of phospho- γ H2AX, 53BP1, and Rad51 to form punctate foci.

The reduction in Rad51 foci formation in gemcitabine treated cells depleted of VDR suggested an impairment in HR. To functionally test whether HR has been compromised after VDR knockdown, we compared the sensitivity of parental and VDR knockdown cells to the PARP inhibitor Rucaparib. This is based on the observation that PARP inhibitors selectively kill BRCA1 defective cells because of their HR deficiency.⁷⁰⁻⁷² Furthermore, PARP inhibition has been shown to increase Rad51 foci,⁷³ and depletion of Rad51 sensitized cells to PARP inhibition.⁴⁰ BxPC3 and Panc1 cells were transfected with control, VDR, and BRCA1 siRNAs and their sensitivity to Rucaparib treatment was compared by clonogenic survival. The results clearly showed that VDR knockdown rendered both cell lines more sensitive to Rucaparib than the controls. For BxPC3 cells, the IC50s after knockdown of BRCA1 and VDR were 1 and 5 μ M, respectively (Fig. 6A) compared to the control IC50 of 9 μ M. For Panc1 cells, the IC50s after knockdown of BRCA1 and VDR were 3.5 and 400 nM, respectively (Fig. 4A) compared to the control (IC50 = 4 μ M). The difference in sensitivities to Rucaparib between VDR and BRCA1 knockdown was due to the fact that Rad51 foci formation was more efficiently inhibited in BRCA1 depleted cells (Figure S6). The increased sensitivity of cells depleted of VDR to Rucaparib supports the data that suggests Rad51 mediated HR functions are impaired.

As VDR is a transcription factor, it may regulate the expression of DNA repair genes such as Rad51 and γ H2AX. Comparison of the levels of these 2 proteins between parental and after VDR knockdown did not show a significant difference that would account for the reduced ability to form DNA damage foci induced by gemcitabine. Western blots were performed to assay VDR's role in regulating the expression of γ H2AX, 53BP1, and Rad51 after DNA damage induction. Parental and BxPC3 VDRkd cells treated with gemcitabine for 18 hours expressed equivalent amounts of Rad51 and H2AX in whole cell extracts (supernatants) (Fig. 6B). However, analysis of the chromatin fractions showed very low amounts of Rad51 and phospho- γ H2AX in VDRkd cells compared to the parental BxPC3 cells (Fig. 6B). This supported our staining data that Rad51 and phospho- γ H2AX foci formation were impaired in VDR depleted cells treated with gemcitabine. To further examine if VDR might be regulating the expression of these and other DNA damage response genes, we used RNAseq to compare the transcriptomes of BxPC3 parental and VDRkd cells of Rad51 and H2AX. This analysis did not identify significant differences in their mRNA levels though the transcript numbers were slightly (<2 fold)

reduced in the BxPC3 VDRkd cells compared to the parental BxPC3 cells (Table S2). We argue that this is not a significant difference as it did not noticeably affect the amount of the proteins.

Rad51 foci formation has been shown to depend on histone acetylation. The histone acetyltransferases TIP48, 49, and 60 have been shown to modulate Rad51 foci formation in response to DNA damage through histone acetylation.^{74,75} Given that VDR forms complexes with coactivators that contain histone acetylases and corepressors that contain HDACs,⁷⁶ it may use this activity to specify Rad51 foci formation. We therefore treated VDRkd cells with the HDAC inhibitor, Trichostatin A (TSA) (500 nM), and monitored Rad51 foci formation after gemcitabine treatment (50 nM) (Fig. 6C) In the absence of TSA, 11% of the VDRkd cells exhibited Rad51 foci after 4 hrs in gemcitabine as compared to 89% positive cells after TSA treatment. This increase was comparable to parental cells where 92% of the cells exhibited Rad51 foci within 4 hours of gemcitabine treatment.

To test the functional relevance of the TSA mediated Rad51 foci formation in the VDR knockdown cells, we tested if TSA altered the sensitivity to gemcitabine. Using the same concentration of TSA (500 nM) that restored the kinetics of Rad51 foci formation, it did not render the VDRkd cells more sensitive to gemcitabine than cells without TSA treatment (both treatments had an IC50 of 50 nM of gemcitabine) (Fig. 6D). Interestingly, parental cell sensitivity to gemcitabine was increased by TSA treatments at the concentrations tested ($p = 0.02$). The IC50 for the gemcitabine plus TSA treated cells was 100 nM compared to cells treated with gemcitabine alone which had an IC50 of ~200 nM (Fig. 6D).

We next wanted to test the contribution of the p300 HAT (histone acetyltransferase)⁷⁷ in Rad51 foci formation given that p300 interacts with VDR to activate transcription of specific target genes.⁷⁸ p300 also has been shown to directly promote Rad51 transcription following DSB induction in lung cancer cell lines.⁷⁹ First, we depleted p300 from BxPC3 and Panc1 cells using shRNAs, and treated cells with gemcitabine and monitored Rad51 foci formation over time. The number of Rad51 foci and overall intensity was reduced in the p300 shRNA transfected cells compared to control cells (Fig. 7A). Of the BxPC3 cells transfected with p300 shRNA, ~22% were positive for Rad51 foci (>5 foci/nucleus) compared to ~84% of the control cells 18 hrs post gemcitabine treatment. Overall Rad51 focal intensity was also reduced by ~35% in the p300 knockdown cells compared to control cells. We also tested for gemcitabine sensitivity after p300 knockdown (Fig. 7B). Consistent with the decreased Rad51 foci, p300 knockdown effectively sensitized BxPC3 cells to gemcitabine. The control shRNA treated cells had an IC50 of

Figure 3 (See previous page). VDR knockdown reduces gemcitabine induced γ H2AX and Rad51 foci formation in BxPC3 and Panc1 cells. (A) Cells were treated with 50 nM gemcitabine, fixed at 0, 2 hrs, 3 hrs, 4 hrs, 6 hrs, 8 hrs, and 18 hrs and stained for Rad51, γ H2AX, and 53BP1. Representative images (40X) from 0, 4, 8 and 18 hrs post drug treatments are shown. (B) Higher magnification (90x) confocal images of individual nuclei displaying the different staining patterns of Rad51, γ H2AX, and 53BP1 after VDR knockdown compared to controls. Percentages of each pattern from 500 cells/sample analyzed are presented.

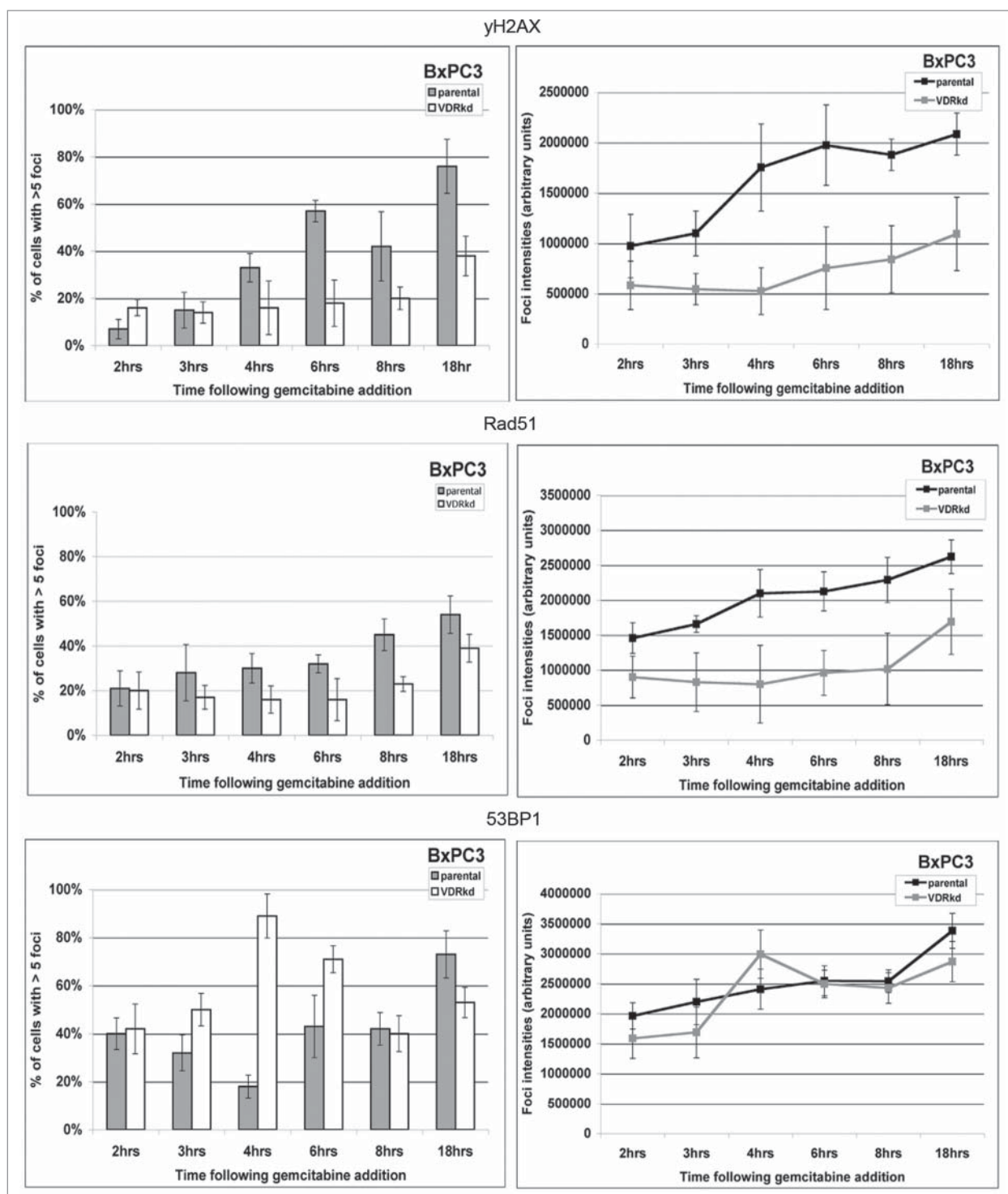


Figure 4. Quantification of Rad51, γ H2AX, and 53BP1 staining of BxPC3 cells. Individual nuclei from images in **Figure 3** were separately analyzed for foci number and focal intensity. Quantitation was performed on cells treated with gemcitabine for 0, 2 hrs, 3 hrs, 4 hrs, 6 hrs, 8 hrs, and 18 hrs. 500 cells from each timepoint was examined for Rad51, γ H2AX, and 53BP1.

~80 nM while the p300 shRNA treated cells had an IC50 of ~40 nM ($p = 0.0489$). Panc1 cells also did not exhibit increased sensitivity to gemcitabine following p300 knockdown with the IC50s of p300 knockdown cells and control cells being similar at

~16 nM and ~19 nM, respectively. This lack of sensitivity maybe due to the fact that Panc1 cells express high basal levels of p300, so RNAi was not sufficient to deplete p300 to levels that altered drug sensitivity.

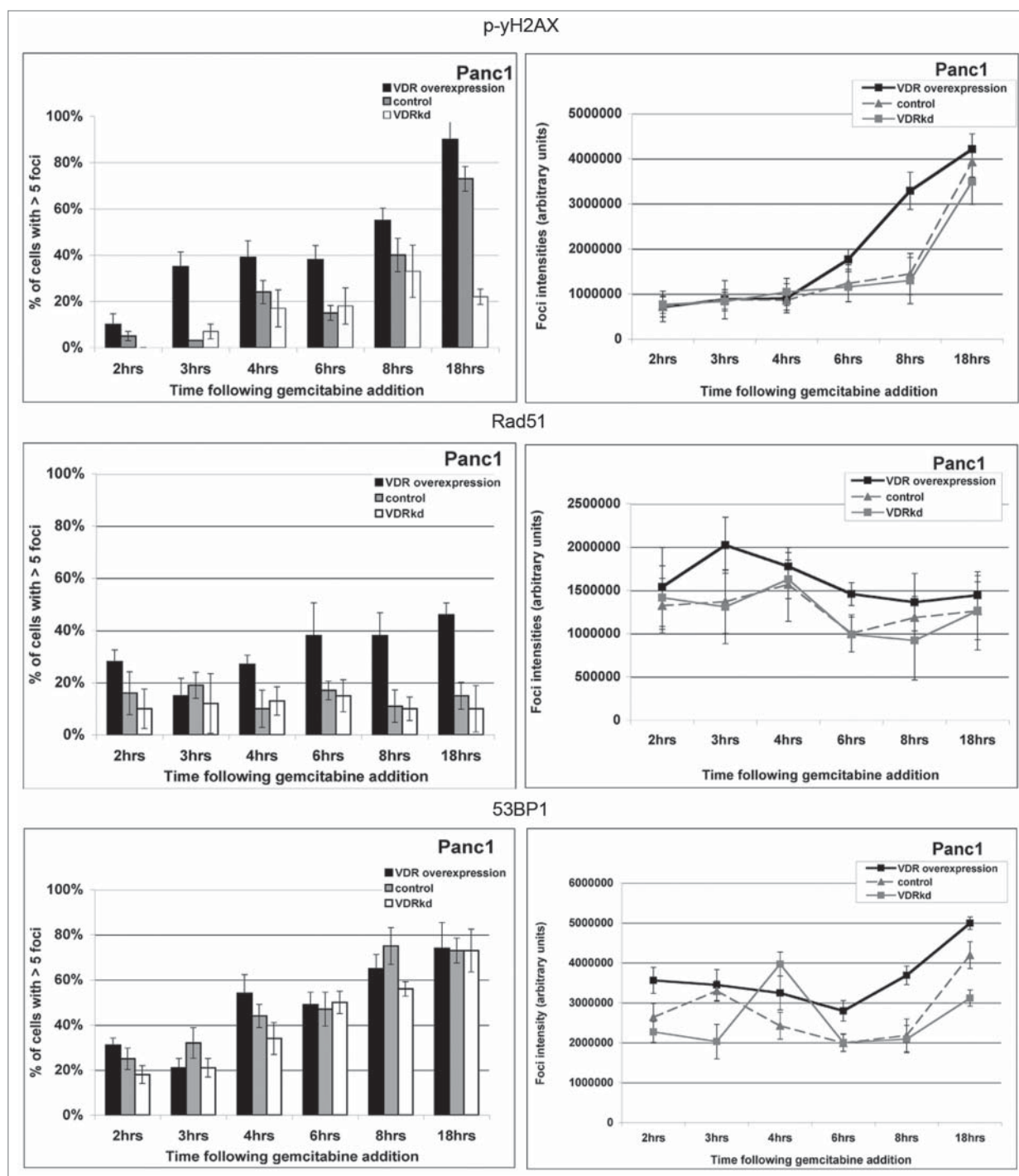


Figure 5. Quantification of Rad51, γ H2AX, and 53BP1 staining of Panc 1 cells. Individual nuclei from images in **Figure 3** were separately analyzed for foci number and focal intensity. Quantitation was performed on cells treated with gemcitabine for 0, 2 hrs, 3 hrs, 4 hrs, 6 hrs, 8 hrs, and 18 hrs. 500 cells from each timepoint was examined for Rad51, γ H2AX, and 53BP1.

Discussion

Our synthetic lethal screen identified 27 target genes that contributed to gemcitabine survival in Panc1 cells. Analysis by STRING and Ingenuity identified 2 networks that specified gemcitabine survival. One was the DNA damage response

network that consisted of CHK1, Wee1, PIAS4, and 53BP1. These genes validated our screen as they have previously been shown to be important for gemcitabine sensitivity as well as other genotoxic drugs.^{42-45,65,80} VDR was part of a second network that also included SRF, and MMP13. Interestingly, Runx2, a VDR binding partner and transcription factor,

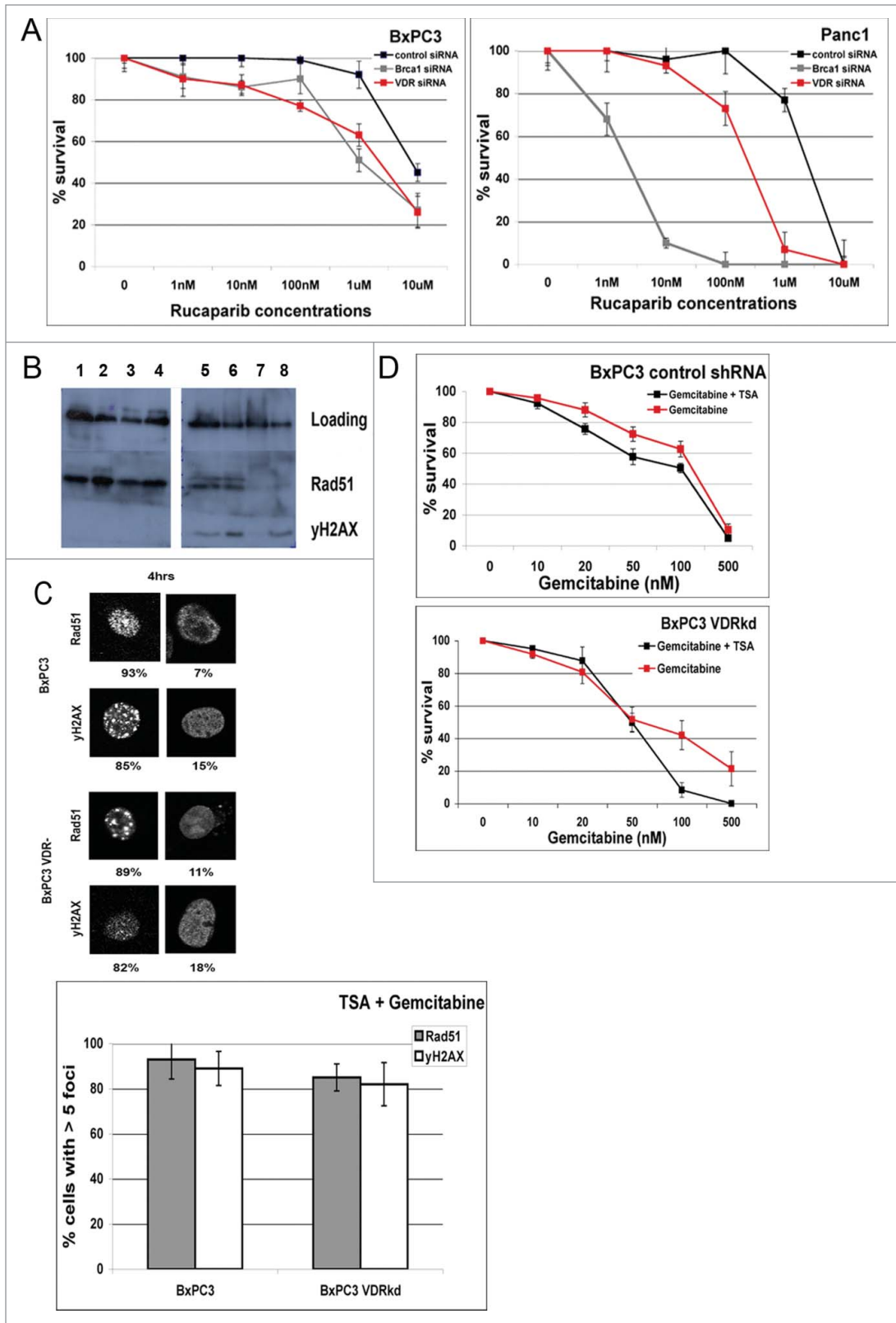


Figure 6. For figure legend, see page 3850.

activates the MMP13 gene during prostate cancer invasion and metastasis.⁸¹ Similarly, RXR α , a major VDR binding partner, directly interacts with SRF and has been shown to compete with SRF for other binding partners like SRC-1 and p300.⁸² We were unable to identify relationships among the remainder 21 genes and these were not assigned to any networks using String DB or Ingenuity. We identified an acetylcholinesterase (ACHE), a dehydrogenase (BCKDHB), phosphatases (DUSP23 and EPM2A), a transferase (GSTM3), a member of the pyruvate dehydrogenase complex (PDHA1), serine/threonine kinase (STK39), a cysteine peptidase (APG4D), a transporter (TNPO2), and transcriptional regulators (TBX4, TBX5, and KLF10). The roles of these genes in gemcitabine sensitization remains to be further investigated.

We focused on VDR because it is a novel target for gemcitabine sensitization, and its knockdown enhanced gemcitabine killing as effectively as with Chk1 knockdown. However, the mechanism of sensitization is not via checkpoint override but rather to a previously unknown role of VDR in Rad51 mediated DNA repair. Our studies showed that VDR is required for the recruitment of Rad51, a key protein in error-free homologous recombination (HR)⁸³ and is a critical determinant of gemcitabine sensitivity because of its importance to repairing stalled replication forks.^{64,65}

We showed that the levels of VDR varied among Panc1, BxPC3 and CFPAC cells, and cells with higher levels were more resistant to gemcitabine. For all the cell lines, knockdown of VDR increased their sensitivity to gemcitabine. BxPC3 cells which were most resistant to gemcitabine (IC₅₀ ~200 nM) showed the greatest reduction (~3-fold) in IC₅₀ after depletion of VDR. Transfection of wild type VDR into the VDR depleted BxPC3 cells increased the IC₅₀ ~6-fold over vector controls, and to levels seen for the parental BxPC3 cells. Consistent with this observation, increasing VDR levels in Panc1 cells (which has less VDR than BxPC3 cells) increased their IC₅₀ to gemcitabine by ~10-fold over controls.

The effects of VDR on gemcitabine sensitivity is ligand and dimerization dependent as VDR mutants lacking these activities failed to rescue the gemcitabine sensitivity of cells depleted of VDR. Furthermore, dominant negative mutants such as VDR S237M and the AML1/ETO oncogene fusion, both of which have been shown to sequester VDR from its partners such as RXR and Runx2^{58,59,84} failed to rescue gemcitabine sensitivity. Despite the ligand dependence for gemcitabine survival, it is unclear if VD3 (1,25 dihydroxyvitamin D) is the ligand. Our studies were conducted using charcoal stripped and dialyzed

serum that does not support VDR dependent transcription in the absence of an exogenous source of ligand.⁸⁵ It is known that VDR can bind other ligands such as curcumin⁸⁶ and lithocholic acid,⁸⁷ the latter which is a toxic bile acid that activates VDR-dependent transcription of the CYP3A detoxifying gene that is independent of VD3. However, it remains formally possible that trace amounts of VD3 in our medium is sufficient to facilitate VDR dependent repair functions.

We showed that VDR was essential for pancreatic cancer cells to form Rad51 and foci in response to gemcitabine. In BxPC3 cells that expressed the highest levels of VDR, Rad51 and phospho- γ H2AX foci form 8 and 4 hours respectively, after addition of gemcitabine and the number and intensity of foci increase for up to 18 hours. In Panc1 cells which have lower VDR levels, or when VDR was experimentally depleted from BxPC3 cells, the kinetics of Rad51 and phospho- γ H2AX foci formation was delayed by 4 and 6 hours respectively, and the intensity of the foci was reduced 1.5 and 2 fold respectively, and never reached the levels seen in control cells. Furthermore, the diffuse staining pattern of Rad51 and phospho- γ H2AX that is seen in the nuclei of VDR depleted cells has been interpreted to reflect catastrophic amounts of DNA damage.⁶⁷ In support of our hypothesis that VDR facilitates Rad51 dependent homologous recombination, both BxPC3 and Panc1 cells were sensitized to the PARP inhibitor Rucaparib after VDR knockdown when compared to control cells. We also observed that the levels of VDR negatively correlated with Rucaparib sensitivity as Panc1 cells (which has less VDR) were more sensitive to Rucaparib than BxPC3 cells. Our data suggest that the level of VDR expression maybe a critical determinant of HR repair efficiency in PCa cells and thus maybe used as a predictive marker for PARP inhibitors.

The mechanism by which VDR facilitates Rad51 foci formation does not appear to be at the level of transcription. Cells depleted of VDR expressed Rad51 protein at levels comparable to control cells. This was corroborated by RNAseq data which showed no significant difference in mRNA levels of not only Rad51 but many of the proteins that are known to be important for Rad51 foci formation (Table S3). The defect lies at the level of recruitment of Rad51 to sites of damage. The defect may be at the level of histone acetylation which is known to be important for Rad51 formation.^{88,89} Indeed, we can rescue Rad51 foci formation in VDR depleted cells with an HDAC inhibitor (TSA) as has been reported by others.^{75,90-92} However, TSA did not increase gemcitabine resistance as it may exert other effects that are toxic to cells. Conversely, when the p300 HAT was depleted

Figure 6 (See previous page). VDR knockdown sensitizes BxPC3 and Panc1 cells to the PARP inhibitor, Rucaparib. blocks gemcitabine induced DSB HR repair by reducing Rad51 foci formation at DSBs. (A) Rucaparib kill curves generated from clonogenic assays of cells transfected with control, BRCA1 and VDR siRNAs. (B) Western blot comparing Rad51 and γ H2AX protein levels of BxPC3 and BxPC3 VDRkd cells. 40 μ g of protein loaded. Lane 1 = BxPC3 + vehicle (18 hrs) (supernatant fraction); Lane 2 = BxPC3 + gemcitabine (50 nM) (18 hrs) (supernatant fraction); Lane 3 = BxPC3 VDRkd + vehicle (18 hrs) (supernatant fraction); Lane 4 = BxPC3 VDRkd + gemcitabine (50 nM) (18 hrs) (supernatant fraction); Lane 5 = BxPC3 + vehicle (18 hrs) (pellet fraction); Lane 6 = BxPC3 + gemcitabine (50 nM) (18 hrs) (pellet fraction); Lane 7 = BxPC3 VDRkd + vehicle (18 hrs) (pellet fraction); Lane 8 = BxPC3 VDRkd + gemcitabine (50 nM) (18 hrs) (pellet fraction). (C) Comparison of Rad51 and γ H2AX staining of BxPC3 and BxPC3kd cells following TSA (500 nM) + gemcitabine (50 nM) treatments. (D) Colony survival of BxPC3 VDRkd and BxPC3 parental cells treated with TSA (500 nM) + gemcitabine (n = 3). p values: BxPC3 VDRkd = 0.289, BxPC3 control = 0.02.

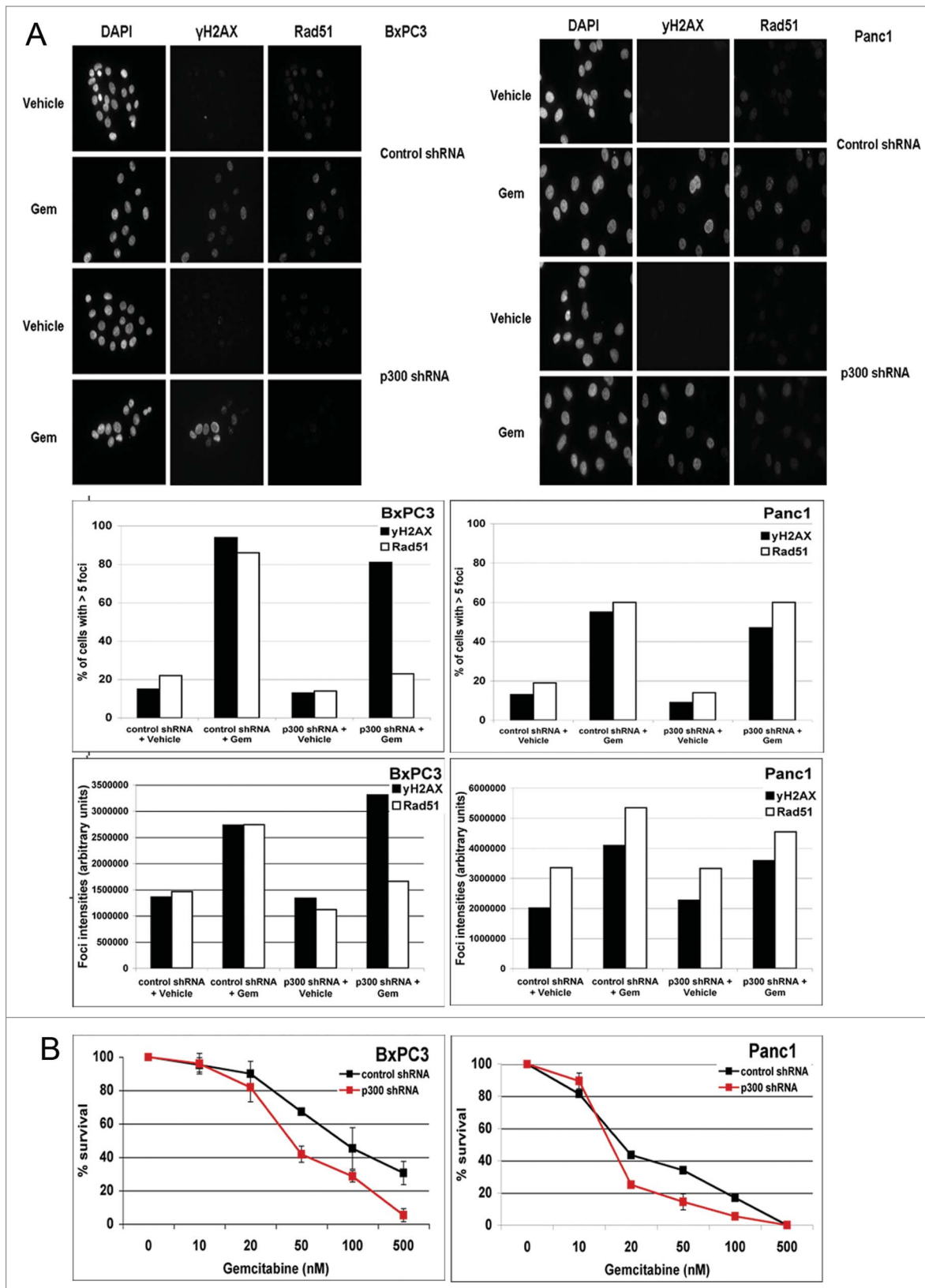


Figure 7. p300 knockdown reduces gemcitabine induced Rad51 foci formation. (A) Rad51 and γ H2AX staining of BxPC3 or Panc1 cells treated with control and p300 shRNA's, and treated with vehicle or gemcitabine. (B) Clonogenic survival assay of BxPC3 and Panc1 cells transfected with p300 shRNA and treated with different doses of gemcitabine (n = 3). p values: BxPC3 = 0.0489, Panc1 = 0.192.

from VDR expressing cells, they failed to form Rad51 foci after gemcitabine treatment. This can explain the increased sensitivity of the p300 knockdown cells to gemcitabine.

We have not tested if VDR plays a similar role in other cancer cells and thus do not know if the relationship between VDR and DNA repair is unique to pancreatic cancer cells. Given that VDR is not an essential gene, we speculate that its role in DNA damage may have evolved in response to increased levels of genomic stress that cells experienced during tumorigenesis.⁹³ In this regard, we cannot say that VDR acts solely in DNA repair because it may also dictate the expression of genes that specify other survival pathways in the cancer cell. As a consequence, VDR became essential for the survival of rapidly dividing PCa cells. This may explain why we were not able to recover stable VDR knockdown cells from Panc1, CFPAC1, and MiaPaca2 cell lines. Thus, targeting VDR alone may be an effective strategy to enhance killing of pancreatic tumor cells in addition to VDR being a chemosensitization target.

Materials and Methods

Cell culture and chemicals

Panc1, BxPC3, and CFPAC1 cells were purchased from American Type Culture Collection (ATCC) and banked at Fox Chase Cancer Center (FCCC) until use. Cell lines were cultured in DMEM/10%FBS supplemented with 2 mM glutamine and 1% penicillin, streptomycin, and kanamycin (PSK) and were maintained at 37°C in 5% CO₂. Charcoal stripped (FCCC cell culture facility) and dialyzed FBS (Life Technologies; 26400-036) were used. Gemcitabine was obtained from the FCCC pharmacy. Rucaparib was a generous gift from N. Johnson (FCCC). Trichostatin A was a generous gift from R. Katz (FCCC).

Plasmids

pLKO.1-VDRshRNA was purchased from Thermo Scientific (TRCN0000019504). pCMV-WT-VDR and pCMV-AML1/ETO plasmids were made from backbones obtained from Addgene. The VDR-S237M mutant was a generous gift from M. Makashima (Nihon University School of Medicine, Tokyo). To create the RNAi resistant allele, pCMV-WT-VDR was mutated at the VDR shRNA target sequence with conservative mutations at the wobble position of 4 consecutive codons. VDR-C288G, K246G, and L254G mutants were created by Quick Change II mutagenesis (Agilent Technologies; 200521).

Synthetic lethal RNAi screen

High throughput RNAi was performed using the validated human genome-wide siRNA library version 2.0 obtained from Dharmacon. This is a SMARTPool (4 siRNAs per gene) library that targeted ~23,500 of the annotated genes, and has been

validated to deplete mRNA by 75%. Stock siRNA was diluted in siRNA buffer (Dharmacon; B-002000-UB-100) and 10 ng of siRNA was reverse transfected into Panc1 cells seeded into white Corning 384-well plates (Fisher Scientific; 07-201-320) in quadruplicates on day 0. Briefly, diluted Dharmafect1 reagent (Dharmacon; T-2001-01) in OptiMEM (Life Technologies; 51985091) was added to the wells and allowed to complex with siRNA for 20 minutes at room temperature. Panc1 cells in 100 μ l of DMEM/10%FBS media without PSK were mixed with 100 μ l of transfection mix at 1000 cells/well. Plates were incubated at 37°C with 5% CO₂. After 48 hours, either vehicle or gemcitabine (50 nM) was added and plates were further incubated for 48 hours. Total viable cell number was determined by the addition of Cell Titer Glo (Promega; G7573) and relative luminescence units (RLU) were measured using an EnVision plate reader (Perkin Elmer). Raw RLU data was normalized to the mean siRNA control on each plate. The effect of gemcitabine treatment on viability was measured based on the normalized viabilities in the drug treated and vehicle wells using Limma.⁹⁴ Statistical significance was measured by p-values controlled for the false discovery rate (FDR) using the Benjamini-Hochberg step-up method⁹⁵ to account for multiple testing. Hits showing an FDR of less than 20% and also a change of at least 15% in viability relative to vehicle treated cells were selected for validation.

RNaseq data analysis

Raw sequence reads were aligned to the human hg19 genome using the Tophat algorithm⁹⁶; Cufflinks algorithm⁹⁷ was implemented to assemble transcripts and estimate their abundance. Cuffdiff⁹⁸ was used to statistically assess expression changes in quantified genes in different conditions.

Cell viability assays

For clonogenic assays, 1000 cells per well were seeded into 6 well plates on day 0. Cells were treated with gemcitabine at various doses on day 1 for 24 hours. Gemcitabine was washed out on day 2, and cells were allowed to grow for a subsequent 10 d before being fixed (10% methanol + 10% acetic acid) and stained with crystal violet (0.4% in 20% ethanol) for colony counting and quantitation as previously described.⁹⁹ For Rucaparib clonogenic assays, the drug was added at various doses 24 hours after cell plating, and cells were allowed to grow for a subsequent 10 d in the presence of Rucaparib. For TSA clonogenic assays, the drug was added for 4 hours prior to addition of gemcitabine or vehicle for another 18 hours before drugs were washed away, and cells were allowed to grow in drug-free medium for 10 d

Microscopy

For timelapse studies, Panc1 cells with stable expression of Histone H2B fused at its C-terminus to GFP were seeded into 6-well plates. Twenty-four hours post cell plating, gemcitabine (50 nM) was added before timelapse was commenced. The plate was placed in a 37C chamber; bright-field and fluorescent images were taken every 5 minutes for 48 hours using a Nikon

TE2000S microscope controlled by Metamorph (Molecular Devices). Three independent movies were conducted for each condition. Movies were allowed to commence for 48 hours for each independent experiment.

For Immunofluorescence, cells were plated onto coverslips 24 hours pre gemcitabine treatment. At different timepoints post gemcitabine treatment, cells were permeabilized, fixed (4% paraformaldehyde) and stained as previously described.⁹⁹ Antibodies to γ H2AX (Millipore; 05–636), Rad51 (a generous gift from G. Ghosal and J. Chen (MD Anderson Cancer Center, Houston, TX), and 53BP1¹⁰⁰ were used. Alexa Fluor-conjugated (488, 555, and 647 nm) secondary antibodies (Molecular probes; A-11029, A-21428, A-21247) were used at a final concentration of 1 μ g/ml and nuclei counterstained with DAPI. Images were captured using a 40X or 63X high NA objective mounted on a semi-automated inverted microscope (Nikon TEi) with a charge-coupled device camera (Photometrics1394) using Nikon Elements 2.0. Exposure times for antibodies were optimized for control samples and identical exposure times used for the experimental samples. Images were quantitated and analyzed using Nikon Elements 2.0. Confocal images were taken using a Leica TCS-SP8 microscope controlled by LAS software (Leica Microsystems).

Western Blotting

BxPC3, Panc1, and CFPAC1 cells were treated with vehicle or gemcitabine (50 nM) for 18 hrs. Cells were harvested, washed in PBS and lysed in NP40 lysis buffer (1% NP40/PBS/10% glycerol) with protease and phosphatase inhibitors. Protein concentrations were determined with MicroBCA Assay (Pierce Biotechnology; 23224 and 23228) and then SDS sample buffer was added to the lysates. 40 μ g of boiled lysates was separated by SDS-PAGE and then transferred onto Immobilon

P membrane (Millipore; IPVH00010). Antibodies used for immunoblotting were obtained from: VDR (Epitomics; 3277–1), γ H2AX (Upstate Biotechnologies, now Millipore; 05–636), Rad51 (Genetex; GTX70230, gift from J. Chen), p300 (Santa Cruz Biotechnologies; SC-584), and TAO1 kinase (Bethyl Labs; A300–524A). TAO1 was used as a loading control since its expression did not vary in any cell lines or drug treatments.

Disclosure of Potential Conflicts of Interest

No potential conflicts of interest were disclosed.

Acknowledgments

We would like to acknowledge M. Einarson of the HTS Facility for helping us design and conduct the siRNA screens, J. Hittle and N. Mitra for excellent technical assistance, G. Ghosal and J.J. Chen for Rad51 antibodies, N. Johnson for advice and the PARP inhibitor experiments, N. Beeharry, A. Nusseinsweig, J. Brody, A. Bellacosa, and A. Andrews for advice and comments.

Funding

This work was partly supported by NIH CA169706, Core grant CA06927, PA Cure, a generous donation by Mrs. C. Greenberg, and the Bucks County Board of Associates. VB was supported by a Pancreatic Cancer Action Network/AACR postdoctoral fellowship.

Supplemental Material

Supplemental data for this article can be accessed on the publisher's website. <http://www.tandfonline.com/kccy>

References

- Caldas C, Kern SE. K-ras mutation and pancreatic adenocarcinoma. *Int J Pancreatol* 1995; 18:1-6; PMID:7594765
- Jones S, Zhang X, Parsons DW, Lin JC, Leary RJ, Angenendt P, Mankoo P, Carter H, Kamiyama H, Jimeno A, et al. Core signaling pathways in human pancreatic cancers revealed by global genomic analyses. *Science* 2008; 321:1801-6; PMID:18772397; <http://dx.doi.org/10.1126/science.1164368>
- Ko AH, Tempero MA. Treatment of metastatic pancreatic cancer. *J Natl Compr Canc Netw* 2005; 3:627-36; PMID:16194454
- van Heek T, Rader AE, Offerhaus GJ, McCarthy DM, Goggins M, Hruban RH, Wilentz RE. K-ras, p53, and DPC4 (MAD4) alterations in fine-needle aspirates of the pancreas: a molecular panel correlates with and supplements cytologic diagnosis. *Am J Clin Pathol* 2002; 117:755-65; PMID:12090425; <http://dx.doi.org/10.1309/5RQ0-JCQU-5XF2-51LQ>
- Weinstein IB. Cancer. Addiction to oncogenes—the Achilles heel of cancer. *Science* 2002; 297:63-4; PMID:12098689; <http://dx.doi.org/10.1126/science.1073096>
- Deramandt T, Rustgi AK. Mutant KRAS in the initiation of pancreatic cancer. *Biochim Biophys Acta* 2005; 1756:97-101; PMID:16169155
- Feldmann G, Rauenzahn S, Maitra A. In vitro models of pancreatic cancer for translational oncology research. *Expert Opin Drug Discov* 2009; 4:429-43; PMID:20160967; <http://dx.doi.org/10.1517/17460440902821657>
- Rubin LL, de Sauvage FJ. Targeting the Hedgehog pathway in cancer. *Nat Rev Drug Discov* 2006; 5:1026-33; PMID:17139287; <http://dx.doi.org/10.1038/nrd2086>
- Park JK, Ryu JK, Lee JK, Yoon WJ, Lee SH, Kim YT, Yoon YB. Gemcitabine chemotherapy vs. 5-fluorouracil-based concurrent chemoradiotherapy in locally advanced unresectable pancreatic cancer. *Pancreas* 2006; 33:397-402; PMID:17079946; <http://dx.doi.org/10.1097/01.mpa.0000236725.26672.be>
- Moore MJ, Goldstein D, Hamm J, Figer A, Hecht JR, Gallinger S, Au HJ, Murawa P, Walde D, Wolff RA, et al. Erlotinib plus gemcitabine compared with gemcitabine alone in patients with advanced pancreatic cancer: a phase III trial of the National Cancer Institute of Canada Clinical Trials Group. *J Clin Oncol* 2007; 25:1960-6; PMID:17452677; <http://dx.doi.org/10.1200/JCO.2006.07.9525>
- Gourgou-Bourgade S, Bascoul-Mollevi C, Desseigne F, Ychou M, Bouche O, Guimbaud R, Becouarn Y, Adenis A, Raoul JL, Boige V, et al. Impact of FOLFIRINOX compared with gemcitabine on quality of life in patients with metastatic pancreatic cancer: results from the PRODIGE 4/ACCORD 11 randomized trial. *J Clin Oncol* 2013; 31:23-9; PMID:23213101; <http://dx.doi.org/10.1200/JCO.2012.44.4869>
- Gunturu KS, Yao X, Cong X, Thumar JR, Hochster HS, Stein SM, Lacy J. FOLFIRINOX for locally advanced and metastatic pancreatic cancer: single institution retrospective review of efficacy and toxicity. *Med Oncol* 2013; 30:361; PMID:23271209; <http://dx.doi.org/10.1007/s12032-012-0361-2>
- Peddi PF, Lubner S, McWilliams R, Tan BR, Picus J, Sorscher SM, Suresh R, Lockhart AC, Wang J, Menias C, et al. Multi-institutional experience with FOLFIRINOX in pancreatic adenocarcinoma. *JOP* 2012; 13:497-501; PMID:22964956.
- Von Hoff DD, Ervin T, Arena FP, Chiorean EG, Infante J, Moore M, Seay T, Tjuland SA, Ma WW, Saleh MN, et al. Increased survival in pancreatic cancer with nab-paclitaxel plus gemcitabine. *N Engl J Med* 2013; 369:1691-703; PMID:24131140; <http://dx.doi.org/10.1056/NEJMoa1304369>
- Schlabach MR, Luo J, Solimini NL, Hu G, Xu Q, Li MZ, Zhao Z, Smogorzewska A, Sowa ME, Ang XL, et al. Cancer proliferation gene discovery through functional genomics. *Science* 2008; 319:620-4; PMID:18239126; <http://dx.doi.org/10.1126/science.1149200>
- Appels NM, Beijnen JH, Schellens JH. Development of farnesyl transferase inhibitors: a review. *Oncologist* 2005; 10:565-78; PMID:16177281; <http://dx.doi.org/10.1634/theoncologist.10-8-565>
- Feig C, Gopinathan A, Neesse A, Chan DS, Cook N, Tuveson DA. The pancreas cancer microenvironment. *Clin Cancer Res* 2012; 18:4266-76; PMID:

- 22896693; <http://dx.doi.org/10.1158/1078-0432.CCR-11-3114>
18. Olive KP, Jacobetz MA, Davidson CJ, Gopinathan A, McIntyre D, Honess D, Madhu B, Goldgraben MA, Caldwell ME, Allard D, et al. Inhibition of Hedgehog signaling enhances delivery of chemotherapy in a mouse model of pancreatic cancer. *Science* 2009; 324:1457-61; PMID:19460966; <http://dx.doi.org/10.1126/science.1171362>
 19. Rhim AD, Oberstein PE, Thomas DH, Mirek ET, Palermo CF, Sastra SA, Dekleva EN, Saunders T, Becerra CP, Tattersall IW, et al. Stromal elements act to restrain, rather than support, pancreatic ductal adenocarcinoma. *Cancer Cell* 2014; 25:735-47; PMID:24856585; <http://dx.doi.org/10.1016/j.ccr.2014.04.021>
 20. Wu Q, Wang R, Yang Q, Hou X, Chen S, Hou Y, Chen C, Yang Y, Miele L, Sarkar FH, et al. Chemoresistance to gemcitabine in hepatoma cells induces epithelial-mesenchymal transition and involves activation of PDGF-D pathway. *Oncotarget* 2013; 4:1999-2009; PMID:24158561.
 21. Isayev O, Rausch V, Bauer N, Liu L, Fan P, Zhang Y, Gladkikh J, Nwaeburu CC, Mattern J, Mollenhauer M, et al. Inhibition of glucose turnover by 3-bromopyruvate counteracts pancreatic cancer stem cell features and sensitizes cells to gemcitabine. *Oncotarget* 2014; 5:5177-89; PMID:25015789
 22. Dobzhansky T. Genetics of natural populations; recombination and variability in populations of *Drosophila pseudoobscura*. *Genetics* 1946; 31:269-90.
 23. Boone C, Bussey H, Andrews BJ. Exploring genetic interactions and networks with yeast. *Nat Rev Genet* 2007; 8:437-49; PMID:17510664; <http://dx.doi.org/10.1038/nrg2085>
 24. Kaelin WG, Jr. The concept of synthetic lethality in the context of anticancer therapy. *Nat Rev Cancer* 2005; 5:689-98; PMID:16110319; <http://dx.doi.org/10.1038/nrc1691>
 25. Bartz SR, Zhang Z, Burchard J, Imakura M, Martin M, Palmieri A, Needham R, Guo J, Gordon M, Chung N, et al. Small interfering RNA screens reveal enhanced cisplatin cytotoxicity in tumor cells having both BRCA network and TP53 disruptions. *Mol Cell Biol* 2006; 26:9377-86; PMID:17000754; <http://dx.doi.org/10.1128/MCB.01229-06>
 26. Whitehurst AW, Bodemann BO, Cardenas J, Ferguson D, Girard L, Peyton M, Minna JD, Michnoff C, Hao W, Roth MG, et al. Synthetic lethal screen identification of chemosensitizer loci in cancer cells. *Nature* 2007; 446:815-9; PMID:17429401; <http://dx.doi.org/10.1038/nature05697>
 27. Zhang X, Jiang F, Li P, Li C, Ma Q, Nicosia SV, Bai W. Growth suppression of ovarian cancer xenografts in nude mice by vitamin D analogue EB1089. *Clin Cancer Res* 2005; 11:323-8; PMID:15671562
 28. Hong SP, Kim MJ, Jung MY, Jeon H, Goo J, Ahn SK, Lee SH, Elias PM, Choi EH. Biopositive effects of low-dose UVB on epidermis: coordinate upregulation of antimicrobial peptides and permeability barrier reinforcement. *J Invest Dermatol* 2008; 128:2880-7; PMID:18580964; <http://dx.doi.org/10.1038/jid.2008.169>
 29. Kommagani R, Payal V, Kadakia MP. Differential regulation of vitamin D receptor (VDR) by the p53 Family: p73-dependent induction of VDR upon DNA damage. *J Biol Chem* 2007; 282:29847-54; PMID:17716971; <http://dx.doi.org/10.1074/jbc.M703641200>
 30. Tachibana S, Yoshinari K, Chikada T, Toriyabe T, Nagata K, Yamazoe Y. Involvement of Vitamin D receptor in the intestinal induction of human ABCB1. *Drug Metab Dispos* 2009; 37:1604-10; PMID:19460946; <http://dx.doi.org/10.1124/dmd.109.027219>
 31. Kittaka A, Yoshida A, Chiang KC, Takano M, Sawada D, Sakaki T, Chen TC. Potent 19-norvitamin D analogs for prostate and liver cancer therapy. *Future Med Chem* 2012; 4:2049-65; PMID:23157238; <http://dx.doi.org/10.4155/fmc.12.130>
 32. Krishnan AV, Trump DL, Johnson CS, Feldman D. The role of vitamin D in cancer prevention and treatment. *Rheum Dis Clin North Am* 2012; 38:161-78; PMID:22525850; <http://dx.doi.org/10.1016/j.rdc.2012.03.014>
 33. Krishnan AV, Swami S, Feldman D. The potential therapeutic benefits of vitamin D in the treatment of estrogen receptor positive breast cancer. *Steroids* 2012; 77:1107-12; PMID:22801352; <http://dx.doi.org/10.1016/j.steroids.2012.06.005>
 34. Wang JY, Swami S, Krishnan AV, Feldman D. Combination of calcitriol and dietary soy exhibits enhanced anticancer activity and increased hypercalcemic toxicity in a mouse xenograft model of prostate cancer. *Prostate* 2012; 72:1628-37; PMID:22457201; <http://dx.doi.org/10.1002/pros.22516>
 35. Vijayakumar S, Mehta RR, Boerner PS, Packianathan S, Mehta RG. Clinical trials involving vitamin D analogs in prostate cancer. *Cancer J* 2005; 11:362-73; PMID:16259866; <http://dx.doi.org/10.1097/00130404-200509000-00002>
 36. Colston KW, James SY, Ofori-Kuragu EA, Binderup L, Grant AG. Vitamin D receptors and anti-proliferative effects of vitamin D derivatives in human pancreatic carcinoma cells in vivo and in vitro. *Br J Cancer* 1997; 76:1017-20; PMID:9376260; <http://dx.doi.org/10.1038/bjc.1997.501>
 37. Yu WD, Ma Y, Flynn G, Muindi JR, Kong RX, Trump DL, Johnson CS. Calcitriol enhances gemcitabine anti-tumor activity in vitro and in vivo by promoting apoptosis in a human pancreatic carcinoma model system. *Cell Cycle* 2010; 9:3022-9; PMID:20699664; <http://dx.doi.org/10.4161/cc.9.15.12381>
 38. Woloszynska-Read A, Johnson CS, Trump DL. Vitamin D and cancer: clinical aspects. *Best Pract Res Clin Endocrinol Metab* 2011; 25:605-15; PMID:21872802; <http://dx.doi.org/10.1016/j.beem.2011.06.006>
 39. Ting HJ, Yasmin-Karim S, Yan SJ, Hsu JW, Lin TH, Zeng W, Messing J, Sheu TJ, Bao BY, Li WX, et al. A positive feedback signaling loop between ATM and the vitamin D receptor is critical for cancer chemoprevention by vitamin D. *Cancer Res* 2012; 72:958-68; PMID:22207345; <http://dx.doi.org/10.1158/0008-5472.CAN-11-0042>
 40. McCabe N, Turner NC, Lord CJ, Kluzek K, Bialkowska A, Swift S, Giavara S, O'Connor MJ, Tutt AN, Zdzienicka MZ, et al. Deficiency in the repair of DNA damage by homologous recombination and sensitivity to poly(ADP-ribose) polymerase inhibition. *Cancer Res* 2006; 66:8109-15; PMID:16912188; <http://dx.doi.org/10.1158/0008-5472.CAN-06-0140>
 41. Bailey JM, Swanson BJ, Hamada T, Eggers JP, Singh PK, Caffery T, Ouellette MM, Hollingsworth MA. Sonic hedgehog promotes desmoplasia in pancreatic cancer. *Clin Cancer Res* 2008; 14:5995-6004; PMID:18829478; <http://dx.doi.org/10.1158/1078-0432.CCR-08-0291>
 42. Azorsa DO, Gonzales IM, Basu GD, Choudhary A, Arora S, Bisanz KM, Kiefer JA, Henderson MC, Trent JM, Von Hoff DD, et al. Synthetic lethal RNAi screening identifies sensitizing targets for gemcitabine therapy in pancreatic cancer. *J Transl Med* 2009; 7:43; PMID:19519883; <http://dx.doi.org/10.1186/1479-5876-7-43>
 43. Rajeshkumar NV, De Oliveira E, Ottenhof N, Waters J, Brooks D, Demuth T, Shumway SD, Mizuarai S, Hirai H, Maitra A, et al. MK-1775, a potent Wee1 inhibitor, synergizes with gemcitabine to achieve tumor regressions, selectively in p53-deficient pancreatic cancer xenografts. *Clin Cancer Res* 2011; 17:2799-806; PMID:21389100; <http://dx.doi.org/10.1158/1078-0432.CCR-10-2580>
 44. Prevo R, Fokas E, Reaper PM, Charlton PA, Pollard JR, McKenna WG, Muschel PJ, Brunton TB. The novel ATR inhibitor VE-821 increases sensitivity of pancreatic cancer cells to radiation and chemotherapy. *Cancer Biol Ther* 2012; 13:1072-81; PMID:22825331; <http://dx.doi.org/10.4161/cbt.21093>
 45. Jena S, Lee WP, Doherty D, Thompson PD. PIAS4 represses vitamin D receptor-mediated signaling and acts as an E3-SUMO ligase towards vitamin D receptor. *J Steroid Biochem Mol Biol* 2012; 132:24-31; PMID:22564762; <http://dx.doi.org/10.1016/j.jsbmb.2012.04.006>
 46. Lal S, Burkhart RA, Beeharry N, Bhattacharjee V, Londin ER, Cozzitorto JA, Romeo C, Jimbo M, Norris ZA, Yeo CJ, et al. HuR posttranscriptionally regulates WEE1: implications for the DNA damage response in pancreatic cancer cells. *Cancer Res* 2014; 74:1128-40; PMID:24536047; <http://dx.doi.org/10.1158/0008-5472.CAN-13-1915>
 47. Menezes RJ, Cheney RT, Husain A, Tretiakova M, Loewen G, Johnson CS, Jayaprakash V, Moysich KB, Salgia R, Reid ME. Vitamin D receptor expression in normal, premalignant, and malignant human lung tissue. *Cancer Epidemiol Biomarkers Prev* 2008; 17:1104-10; PMID:18483332; <http://dx.doi.org/10.1158/1055-9965.EPI-07-2713>
 48. Qi X, Tang J, Pramanik R, Schultz RM, Shirasawa S, Sasazuki T, Han J, Chen G. p38 MAPK activation selectively induces cell death in K-ras-mutated human colon cancer cells through regulation of vitamin D receptor. *J Biol Chem* 2004; 279:22138-44; PMID:15037631; <http://dx.doi.org/10.1074/jbc.M313964200>
 49. Teichert AE, Elalieh H, Elias PM, Welsh J, Bikle DD. Overexpression of hedgehog signaling is associated with epidermal tumor formation in vitamin D receptor-null mice. *J Invest Dermatol* 2011; 131:2289-97; PMID:21814234; <http://dx.doi.org/10.1038/jid.2011.196>
 50. Sequeira VB, Rybchyn MS, Tongkoo-On W, Gordon-Thomson C, Malloy PJ, Nemere I, Norman AW, Reeve VE, Halliday GM, Feldman D, et al. The role of the vitamin D receptor and ERp57 in photoprotection by 1alpha,25-dihydroxyvitamin D3. *Mol Endocrinol* 2012; 26:574-82; PMID:22322599; <http://dx.doi.org/10.1210/me.2011-1161>
 51. Beeharry N, Rattner JB, Caviston JP, Yen T. Centromere fragmentation is a common mitotic defect of S and G2 checkpoint override. *Cell Cycle* 2013; 12:1588-97; PMID:23624842; <http://dx.doi.org/10.4161/cc.24740>
 52. Busby EC, Leistritz DF, Abraham RT, Karnitz LM, Sarkaria JN. The radiosensitizing agent 7-hydroxytaurosporine (UCN-01) inhibits the DNA damage checkpoint kinase hChk1. *Cancer Res* 2000; 60:2108-12; PMID:10786669
 53. Graves PR, Yu L, Schwarz JK, Gales J, Sausville EA, O'Connor PM, Piwnicka-Worms H. The Chk1 protein kinase and the Cdc25C regulatory pathways are targets of the anticancer agent UCN-01. *J Biol Chem* 2000; 275:5600-5; PMID:10681541; <http://dx.doi.org/10.1074/jbc.275.8.5600>
 54. Zhao H, Watkins JL, Piwnicka-Worms H. Disruption of the checkpoint kinase 1/cell division cycle 25A pathway abrogates ionizing radiation-induced S and G2 checkpoints. *Proc Natl Acad Sci U S A* 2002; 99:14795-800; PMID:12399544; <http://dx.doi.org/10.1073/pnas.182557299>
 55. Zabludoff SD, Deng C, Grondine MR, Sheehy AM, Ashwell S, Caleb BL, Green S, Haye HR, Horn CL, Janetka JW, et al. AZD7762, a novel checkpoint kinase inhibitor, drives checkpoint abrogation and potentiates DNA-targeted therapies. *Mol Cancer Ther* 2008; 7:2955-66; PMID:18790776; <http://dx.doi.org/10.1158/1535-7163.MCT-08-0492>
 56. Blasina A, Hallin J, Chen E, Arango ME, Kraynov E, Register J, Grant S, Ninkovic S, Chen P, Nichols T, et al. Breaching the DNA damage checkpoint via PF-00477736, a novel small-molecule inhibitor of checkpoint kinase 1. *Mol Cancer Ther* 2008; 7:2394-404; PMID:18723486; <http://dx.doi.org/10.1158/1535-7163.MCT-07-2391>

57. Sicinska W, Rotkiewicz P, DeLuca HF. Model of three-dimensional structure of VDR bound with Vitamin D3 analogs substituted at carbon-2. *J Steroid Biochem Mol Biol* 2004; 89-90:107-10; PMID: 15225755.
58. Adachi R, Shulman AI, Yamamoto K, Shimomura I, Yamada S, Mangelsdorf DJ, Makishima M. Structural determinants for vitamin D receptor response to endocrine and xenobiotic signals. *Mol Endocrinol* 2004; 18:43-52; PMID:14525957; <http://dx.doi.org/10.1210/me.2003-0244>
59. Shen Q, Christakos S. The vitamin D receptor, Runx2, and the Notch signaling pathway cooperate in the transcriptional regulation of osteopontin. *J Biol Chem* 2005; 280:40589-98; PMID:16195230; <http://dx.doi.org/10.1074/jbc.M504166200>
60. Fazi F, Racanicchi S, Zardo G, Starnes LM, Mancini M, Travaglini L, Diverio D, Ammatuna E, Cimino G, Lo-Coco F, et al. Epigenetic silencing of the myelopoiesis regulator microRNA-223 by the AML1/ETO oncoprotein. *Cancer Cell* 2007; 12:457-66; PMID:17996649; <http://dx.doi.org/10.1016/j.ccr.2007.09.020>
61. Huang X, Tran T, Zhang L, Hatcher R, Zhang P. DNA damage-induced mitotic catastrophe is mediated by the Chk1-dependent mitotic exit DNA damage checkpoint. *Proc Natl Acad Sci U S A* 2005; 102:1065-70; PMID:15650047; <http://dx.doi.org/10.1073/pnas.0409130102>
62. Bartucci M, Svensson S, Romania P, Dattilo R, Patrizzi M, Signore M, Navarra S, Loti F, Biffoni M, Pillozzi E, et al. Therapeutic targeting of Chk1 in NSCLC stem cells during chemotherapy. *Cell Death Differ* 2012; 19:768-78; PMID:22117197; <http://dx.doi.org/10.1038/cdd.2011.170>
63. Ewald B, Sampath D, Plunkett W. H2AX phosphorylation marks gemcitabine-induced stalled replication forks and their collapse upon S-phase checkpoint abrogation. *Mol Cancer Ther* 2007; 6:1239-48; PMID:17406032; <http://dx.doi.org/10.1158/1535-7163.MCT-06-0633>
64. Tsai MS, Kuo YH, Chiu YF, Su YC, Lin YW. Down-regulation of Rad51 expression overcomes drug resistance to gemcitabine in human non-small-cell lung cancer cells. *J Pharmacol Exp Ther* 2010; 335:830-40; PMID:20855443; <http://dx.doi.org/10.1124/jpet.110.173146>
65. Parsels LA, Morgan MA, Tanska DM, Parsels JD, Palmer BD, Booth RJ, Denny WA, Canman CE, Kraker AJ, Lawrence TS, et al. Gemcitabine sensitization by checkpoint kinase 1 inhibition correlates with inhibition of a Rad51 DNA damage response in pancreatic cancer cells. *Mol Cancer Ther* 2009; 8:45-54; PMID:19139112; <http://dx.doi.org/10.1158/1535-7163.MCT-08-0662>
66. Bunting SF, Callen E, Wong N, Chen HT, Polato F, Gunn A, Bothmer A, Feldhahn N, Fernandez-Capetillo O, Cao L, et al. 53BP1 inhibits homologous recombination in Brca1-deficient cells by blocking resection of DNA breaks. *Cell* 2010; 141:243-54; PMID:20362325; <http://dx.doi.org/10.1016/j.cell.2010.03.012>
67. Celeste A, Fernandez-Capetillo O, Kruhlak MJ, Pilch DR, Staudt DW, Lee A, Bonner RF, Bonner WM, Nussenzweig A. Histone H2AX phosphorylation is dispensable for the initial recognition of DNA breaks. *Nat Cell Biol* 2003; 5:675-9; PMID:12792649; <http://dx.doi.org/10.1038/ncb1004>
68. Tauchi H, Matsuura S, Kobayashi J, Sakamoto S, Komatsu K. Nijmegen breakage syndrome gene, NBS1, and molecular links to factors for genome stability. *Oncogene* 2002; 21:8967-80; PMID:12483513; <http://dx.doi.org/10.1038/sj.onc.1206136>
69. Fragkos M, Jurvanstuu J, Beard P. H2AX is required for cell cycle arrest via the p53/p21 pathway. *Mol Cell Biol* 2009; 29:2828-40; PMID:19273588; <http://dx.doi.org/10.1128/MCB.01830-08>
70. Farmer H, McCabe N, Lord CJ, Tutt AN, Johnson DA, Richardson TB, Santarosa M, Dillon KJ, Hickson I, Knights C, et al. Targeting the DNA repair defect in BRCA mutant cells as a therapeutic strategy. *Nature* 2005; 434:917-21; PMID:15829967; <http://dx.doi.org/10.1038/nature03445>
71. Gallmeier E, Kern SE. Absence of specific cell killing of the BRCA2-deficient human cancer cell line CAPAN1 by poly(ADP-ribose) polymerase inhibition. *Cancer Biol Ther* 2005; 4:703-6; PMID:16082177; <http://dx.doi.org/10.4161/cbt.4.7.1909>
72. McCabe N, Lord CJ, Tutt AN, Martin NM, Smith GC, Ashworth A. BRCA2-deficient CAPAN-1 cells are extremely sensitive to the inhibition of Poly(ADP-Ribose) polymerase: an issue of potency. *Cancer Biol Ther* 2005; 4:934-6; PMID:16251802; <http://dx.doi.org/10.4161/cbt.4.9.2141>
73. Schultz N, Lopez E, Saleh-Gohari N, Helleday T. Poly(ADP-ribose) polymerase (PARP-1) has a controlling role in homologous recombination. *Nucleic Acids Res* 2003; 31:4959-64; PMID:12930944; <http://dx.doi.org/10.1093/nar/gkg703>
74. Gospodinov A, Tsaneva I, Anachkova B. RAD51 foci formation in response to DNA damage is modulated by TIP49. *Int J Biochem Cell Biol* 2009; 41:925-33; PMID:18834951; <http://dx.doi.org/10.1016/j.biocel.2008.09.004>
75. Murr R, Loizou JI, Yang YG, Cuenin C, Li H, Wang ZQ, Herceg Z. Histone acetylation by Trp-Tip60 modulates loading of repair proteins and repair of DNA double-strand breaks. *Nat Cell Biol* 2006; 8:91-9; PMID:16341205; <http://dx.doi.org/10.1038/ncb1343>
76. Haussler MR, Haussler CA, Bartik L, Whitfield GK, Hsieh JC, Slater S, Jurutka PW. Vitamin D receptor: molecular signaling and actions of nutritional ligands in disease prevention. *Nutr Rev* 2008; 66:S98-112; PMID:18844852; <http://dx.doi.org/10.1111/j.1753-4887.2008.00093.x>
77. Kraus WL, Manning ET, Kadonaga JT. Biochemical analysis of distinct activation functions in p300 that enhance transcription initiation with chromatin templates. *Mol Cell Biol* 1999; 19:8123-35; PMID:10567538
78. Deeb KK, Trump DL, Johnson CS. Vitamin D signaling pathways in cancer: potential for anticancer therapeutics. *Nat Rev Cancer* 2007; 7:684-700; PMID:17721433; <http://dx.doi.org/10.1038/nrc2196>
79. Ogiwara H, Kohno T. CBP and p300 histone acetyltransferases contribute to homologous recombination by transcriptionally activating the BRCA1 and RAD51 genes. *PLoS One* 2012; 7:e52810; PMID:23285190; <http://dx.doi.org/10.1371/journal.pone.0052810>
80. Montano R, Thompson R, Chung I, Hou H, Khan N, Eastman A. Sensitization of human cancer cells to gemcitabine by the Chk1 inhibitor MK-8776: cell cycle perturbation and impact of administration schedule in vitro and in vivo. *BMC Cancer* 2013; 13:604; PMID:24359526; <http://dx.doi.org/10.1186/1471-2407-13-604>
81. Martin JW, Zielenska M, Stein GS, van Wijnen AJ, Squire JA. The Role of RUNX2 in Osteosarcoma Oncogenesis. *Sarcoma* 2011; 2011:282745; PMID:21197465; <http://dx.doi.org/10.1155/2011/282745>
82. Kim SW, Kim HJ, Jung DJ, Lee SK, Kim YS, Kim JH, Kim TS, Lee JW. Retinoid-dependent antagonism of serum response factor transactivation mediated by transcriptional coactivator proteins. *Oncogene* 2001; 20:6638-42; PMID:11641790; <http://dx.doi.org/10.1038/sj.onc.1204695>
83. Vise P, Cazaux C, Lesca C, Defais M. Overexpression of Rad51 protein stimulates homologous recombination and increases resistance of mammalian cells to ionizing radiation. *Nucleic Acids Res* 1998; 26:2859-64; PMID:9611228; <http://dx.doi.org/10.1093/nar/26.12.2859>
84. Puccetti E, Obradovic D, Beisert T, Bianchini A, Washburn B, Chiaradonna F, Bochrer S, Hoelzer D, Ottmann OG, Pelicci PG, et al. AML-associated translocation products block vitamin D(3)-induced differentiation by sequestering the vitamin D(3) receptor. *Cancer Res* 2002; 62:7050-8; PMID:12460926
85. Cao Z, West C, Norton-Wenzel CS, Rej R, Davis FB, Davis PJ, Rej R. Effects of resin or charcoal treatment on fetal bovine serum and bovine calf serum. *Endocr Res* 2009; 34:101-8; PMID:19878070; <http://dx.doi.org/10.3109/07435800903204082>
86. Bartik L, Whitfield GK, Kaczmarek M, Lowmiller CL, Moffet EW, Furmick JK, Hernandez Z, Haussler CA, Haussler MR, Jurutka PW. Curcumin: a novel nutritionally derived ligand of the vitamin D receptor with implications for colon cancer chemoprevention. *J Nutr Biochem* 2010; 21:1153-61; PMID:20153625; <http://dx.doi.org/10.1016/j.jnutbio.2009.09.012>
87. Adachi R, Honma Y, Masuno H, Kawana K, Shimomura I, Yamada S, Makishima M. Selective activation of vitamin D receptor by lithocholic acid acetate, a bile acid derivative. *J Lipid Res* 2005; 46:46-57; PMID:15489543; <http://dx.doi.org/10.1194/jlr.M400294-JLR200>
88. Eberharter A, Becker PB. Histone acetylation: a switch between repressive and permissive chromatin. Second in review series on chromatin dynamics. *EMBO Rep* 2002; 3:224-9; PMID:11882541; <http://dx.doi.org/10.1093/embo-reports/kvf053>
89. Nakatani Y. Histone acetylases—versatile players. *Genes Cells* 2001; 6:79-86; PMID:11260253; <http://dx.doi.org/10.1046/j.1365-2443.2001.00411.x>
90. Calao M, Burny A, Quivy Y, Dekoninck A, Van Lint C. A pervasive role of histone acetyltransferases and deacetylases in an NF-kappaB-signaling code. *Trends Biochem Sci* 2008; 33:339-49; PMID:18585916; <http://dx.doi.org/10.1016/j.tibs.2008.04.015>
91. Quivy Y, Van Lint C. Regulation at multiple levels of NF-kappaB-mediated transactivation by protein acetylation. *Biochem Pharmacol* 2004; 68:1221-9; PMID:15313420; <http://dx.doi.org/10.1016/j.bcp.2004.05.039>
92. Furumai R, Komatsu Y, Nishino N, Khochbin S, Yoshida M, Horinouchi S. Potent histone deacetylase inhibitors built from trichostatin A and cyclic tetrapeptide antibiotics including trapoxin. *Proc Natl Acad Sci U S A* 2001; 98:87-92; PMID:11134513; <http://dx.doi.org/10.1073/pnas.98.1.87>
93. Schwartzman JM, Sotillo R, Benezra R. Mitotic chromosomal instability and cancer: mouse modelling of the human disease. *Nat Rev Cancer* 2010; 10:102-15; PMID:20094045; <http://dx.doi.org/10.1038/nrc2781>
94. Smyth GK. Linear models and empirical bayes methods for assessing differential expression in microarray experiments. *Stat Appl Genet Mol Biol* 2004; 3:Article3; PMID:16646809.
95. Klipper-Aurbach Y, Wasserman M, Braunsiegel-Weintrob N, Borstein D, Peleg S, Assa S, Karp M, Benjamini Y, Hochberg Y, Laron Z. Mathematical formulae for the prediction of the residual beta cell function during the first two years of disease in children and adolescents with insulin-dependent diabetes mellitus. *Med Hypotheses* 1995; 45:486-90; PMID:8748093; [http://dx.doi.org/10.1016/0306-9877\(95\)90228-7](http://dx.doi.org/10.1016/0306-9877(95)90228-7)
96. Trapnell C, Pachter L, Salzberg SL. TopHat: discovering splice junctions with RNA-Seq. *Bioinformatics* 2009; 25:1105-11; PMID:19289445; <http://dx.doi.org/10.1093/bioinformatics/btp120>
97. Trapnell C, Williams BA, Pertea G, Mortazavi A, Kwan G, van Baren MJ, Salzberg SL, Wold BJ, Pachter L. Transcript assembly and quantification by RNA-Seq reveals unannotated transcripts and isoform switching during cell differentiation. *Nat Biotechnol* 2010; 28:511-5; PMID:20436464; <http://dx.doi.org/10.1038/nbt.1621>

98. Trapnell C, Hendrickson DG, Sauvageau M, Goff L, Rinn JL, Pachter L. Differential analysis of gene regulation at transcript resolution with RNA-seq. *Nat Biotechnol* 2013; 31:46-53; PMID:23222703; <http://dx.doi.org/10.1038/nbt.2450>
99. Becharry N, Rattner JB, Bellacosa A, Smith MR, Yen TJ. Dose dependent effects on cell cycle checkpoints and DNA repair by bendamustine. *PLoS One* 2012; 7:e40342; PMID:22768280
100. Kao GD, McKenna WG, Guenther MG, Muschel RJ, Lazar MA, Yen TJ. Histone deacetylase 4 interacts with 53BP1 to mediate the DNA damage response. *J Cell Biol* 2003; 160:1017-27; PMID:12668657; <http://dx.doi.org/10.1083/jcb.200209065>